



Weyl Semimetals



© Nature

Claudia Felser



Co-workers in Dresden and elsewhere



Johannes Gooth, IBM Zürich

Andrei Bernevig, Princeton, PIS ARPES team

Uli Zeitler, et al. HFML - EMFL, Nijmegen; J. Wosnitza et al., HFML Rossendorf

Yulin Chen et al., Oxford; Kornelius Nielsch, IFW Dresden

S. S. P. Parkin et al., IBM Almaden, MPI Halle



Alexander von Humboldt
Stiftung/Foundation



Topology – interdisciplinary



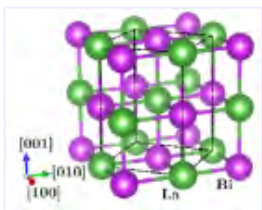
Chemistry

Real space - local
Crystals



LaBi

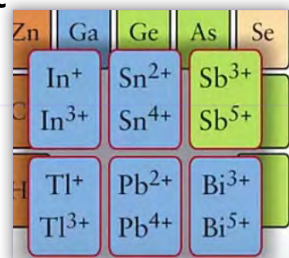
Crystal structure



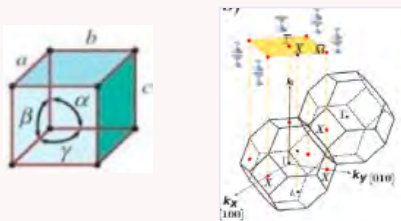
Position of the atoms
Orbitals

Check	WP	Representative
<input type="checkbox"/>	8g	x,y,z
<input type="checkbox"/>	4f	x,1/2,z
<input type="checkbox"/>	4e	x,0,z
<input checked="" type="checkbox"/>	4d	x,x,z
<input checked="" type="checkbox"/>	2c	1/2,0,z
<input type="checkbox"/>	1b	1/2,1/2,z
<input checked="" type="checkbox"/>	1a	0,0,z

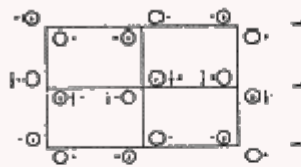
Inert pair effect



Symmetry



Local symmetry

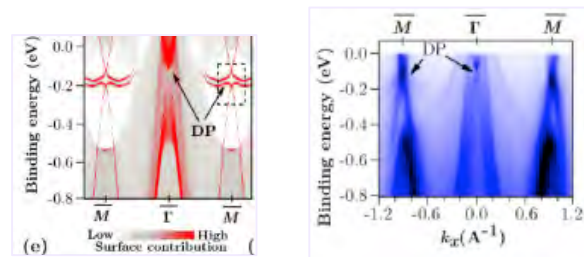


Relativistic effects

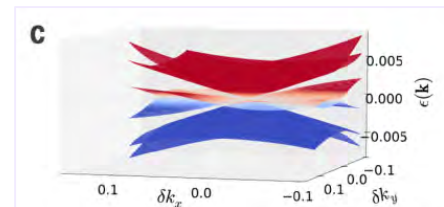
Physics

Recipro. space -deloc
Brillouin zone

Electronic structure



Band connectivity



Darwin term

$$H_{\text{Darwin}} = \frac{\hbar^2}{8m_e^2 c^2} (\Delta V)$$

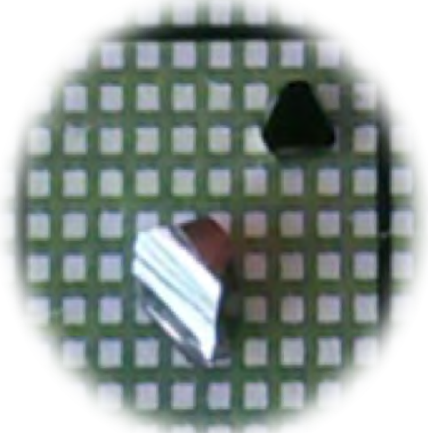


Particles – Universe – Condensed matter

Quantum field theory – Berry curvature

Dirac

Cd_3As_2
Cava, Ong



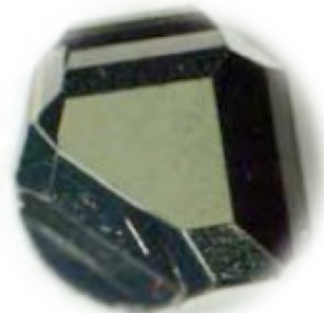
Higgs

YMnO_3
Lichtenberg Spaldin



Weyl

NbP , WP_2
Vicky Süss, Marcus Schmidt



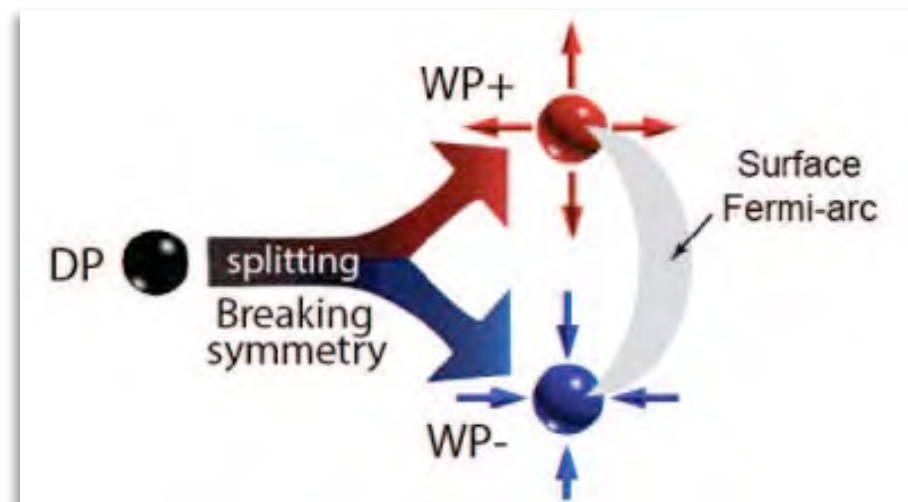
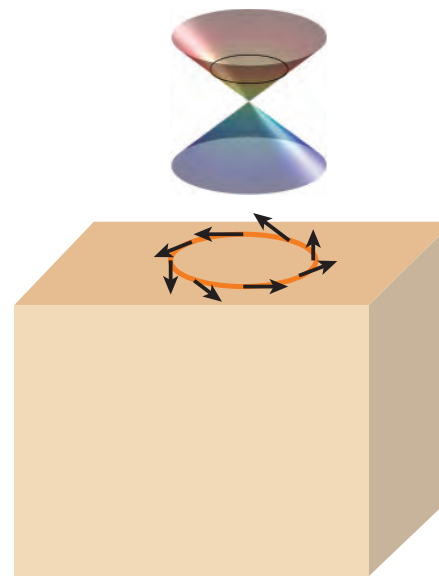
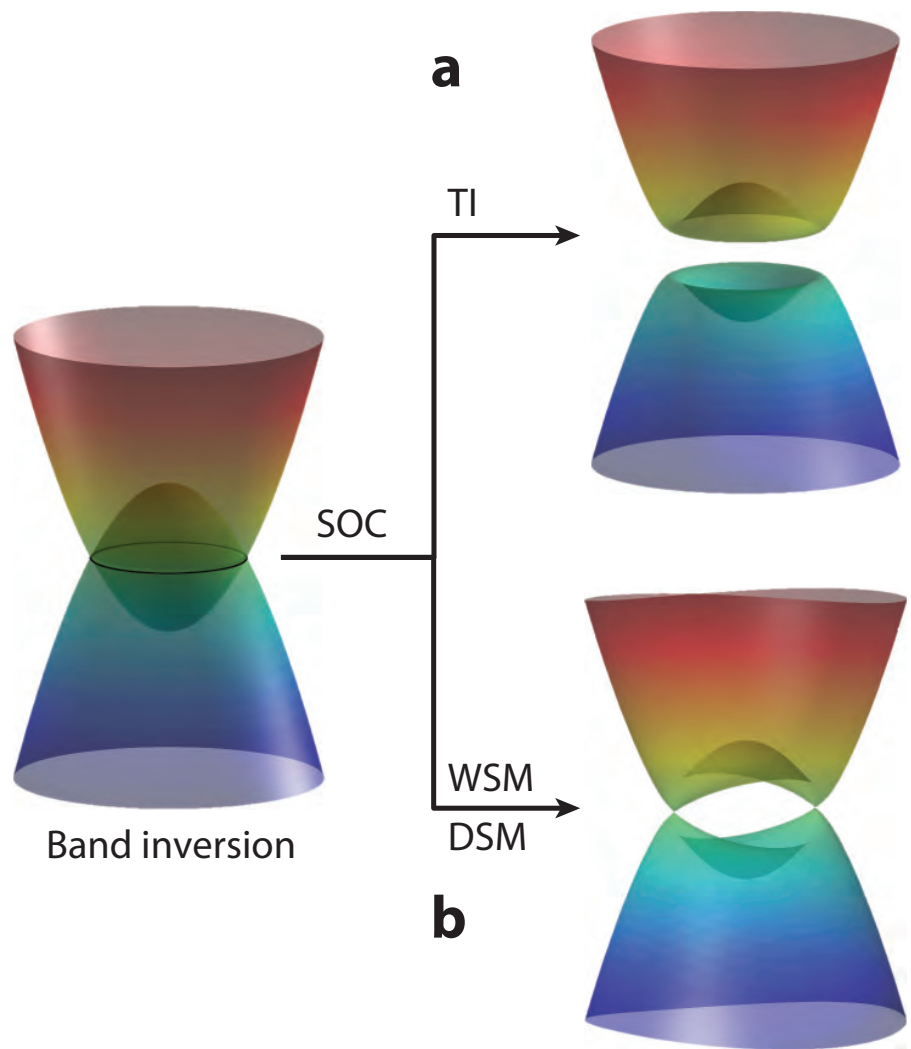
Majorana

YPtBi
Chandra Shekhar



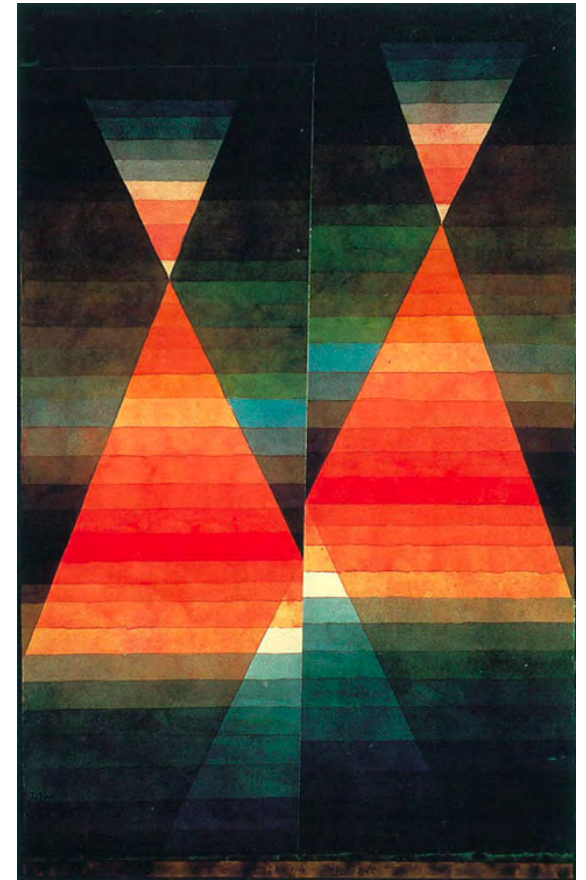


Weyl semimetals





Weyl Semimetals



Paul Klee



Weyl semimetals

3D topological Weyl semimetals - breaking time reversal symmetry – in transport measurement we should see:

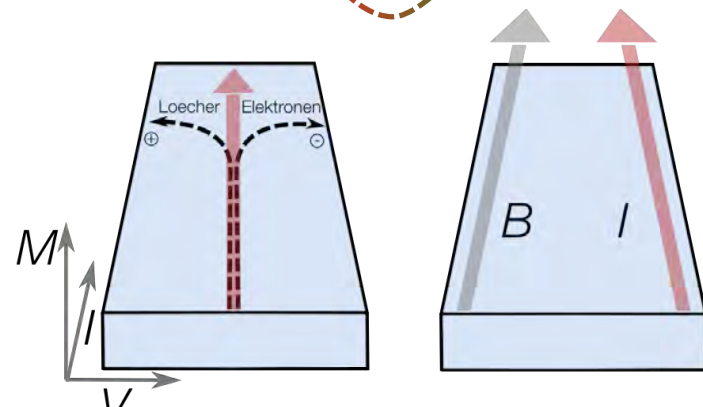
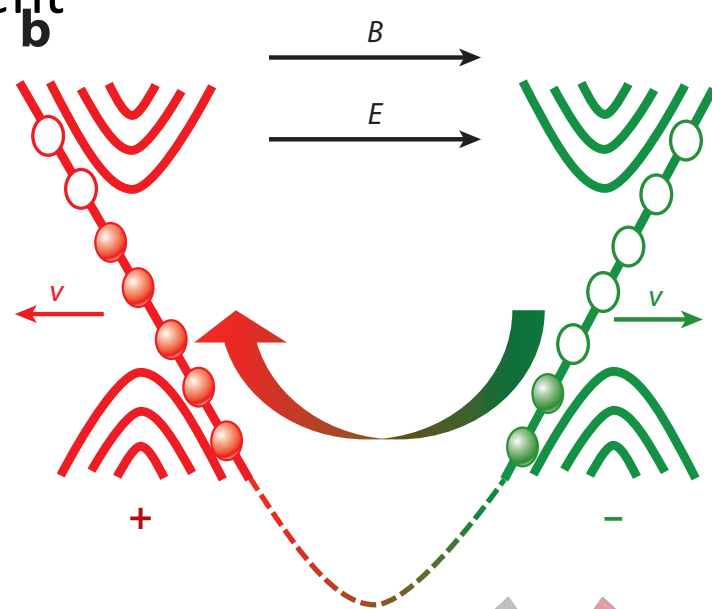
1. Fermi arc



2. Chiral anomaly

$$\partial_\mu j_\chi^\mu = -\chi \frac{e^3}{4\pi^2 \hbar^2} \mathbf{E} \cdot \mathbf{B}$$

$$\sigma_a = \frac{e^3 v_f^3}{4\pi^2 \hbar \mu^2 c} B^2$$



- S. L. Adler, Phys. Rev. 177, 2426 (1969)
- J. S. Bell and R. Jackiw, Nuovo Cim. A60, 47 (1969)
- AA Zyuzin, AA Burkov - Physical Review B (2012)
- AA Burkov, L Balents, PRL 107 12720 (2012)

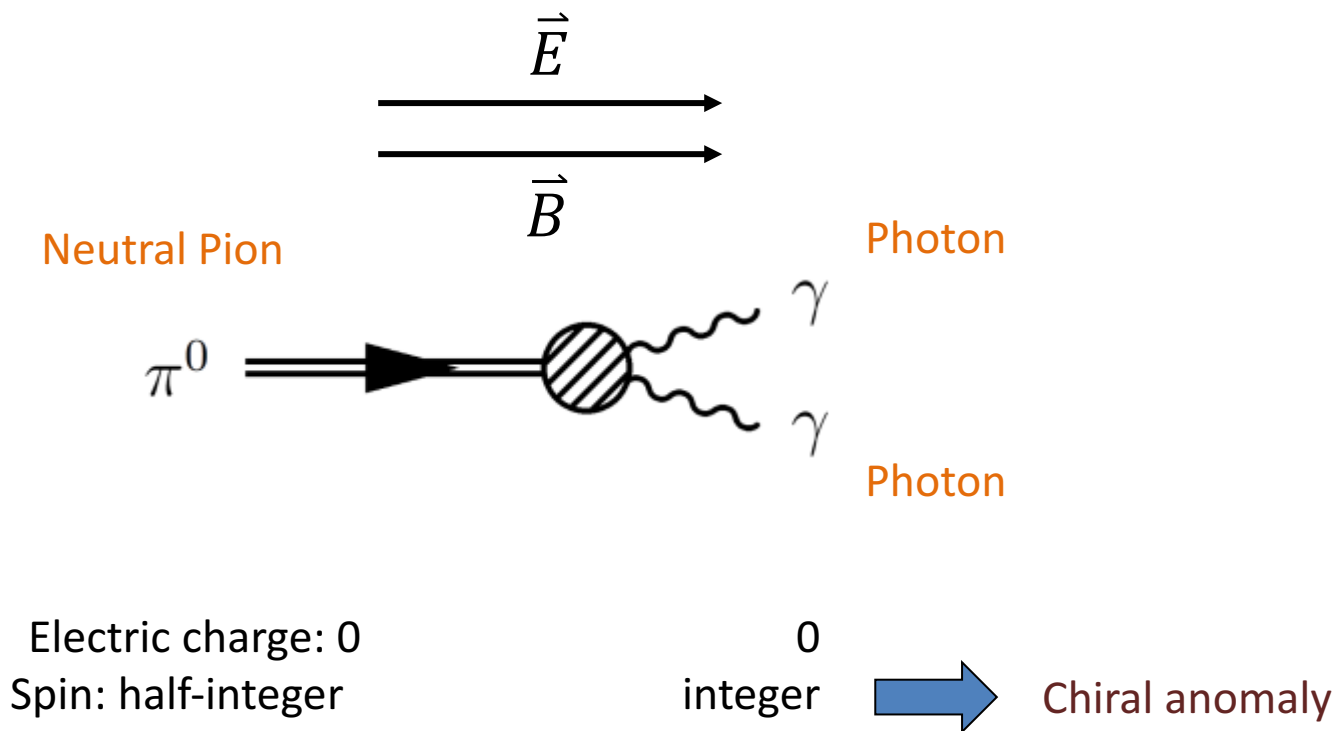


Quantum anomaly in QED

Violation of chiral symmetry.

In Quantum Electro Dynamics (relativistic quantum field theory) chiral charge conservation can be violated for massless fermions!

Pion decay:



Adler, S. L. *Phys. Rev.* **177**, 5 (1969).

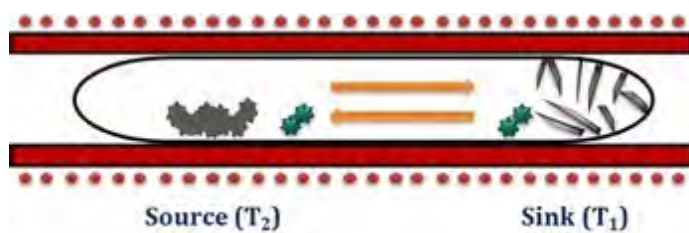
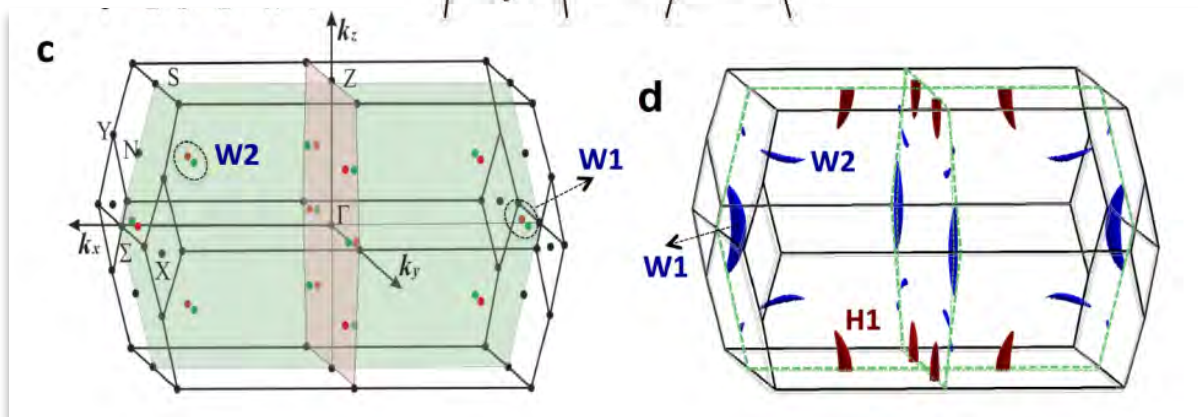
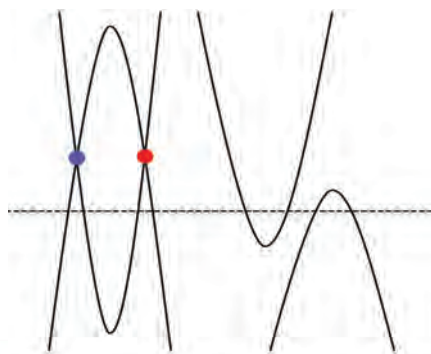
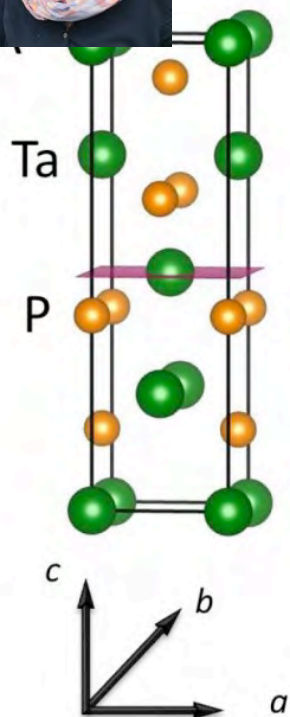
Bell, J. S. & Jackiw, R. *Nuovo Cim.* **A60**, 4 (1969)



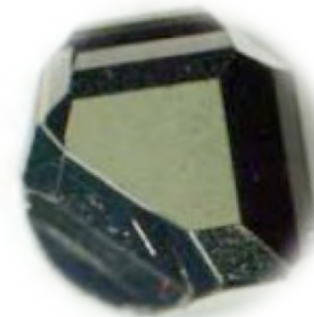
Weyl semimetals in non-centro NbP



NbP, NbAs,
TaP, TaAs



- Transport agent
- Precursor
- Single crystals

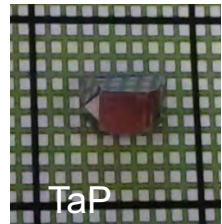
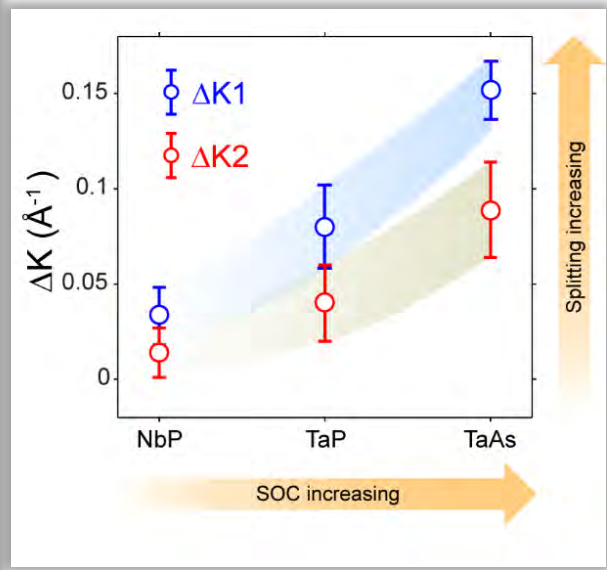
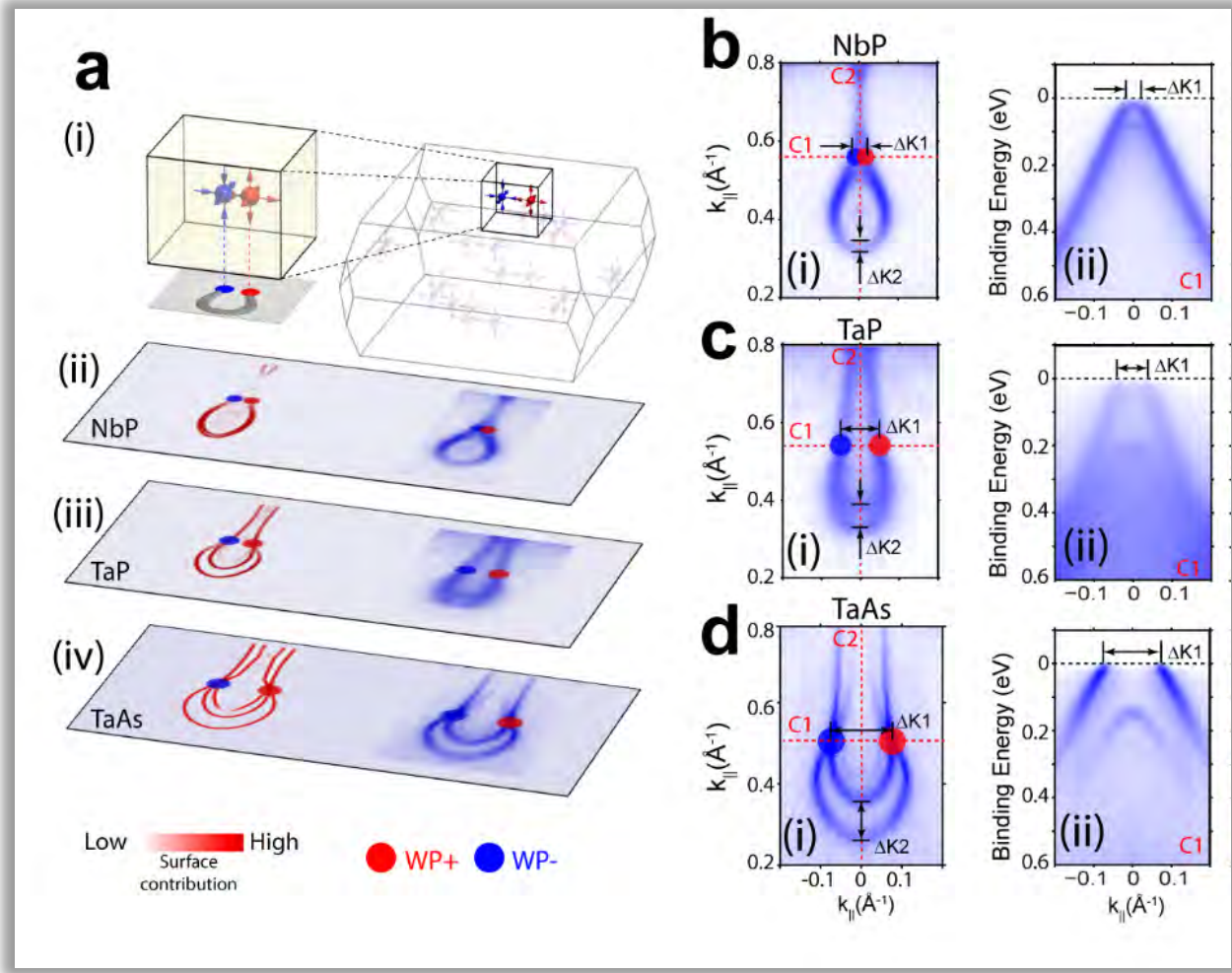




NbP, TaP, TaAs



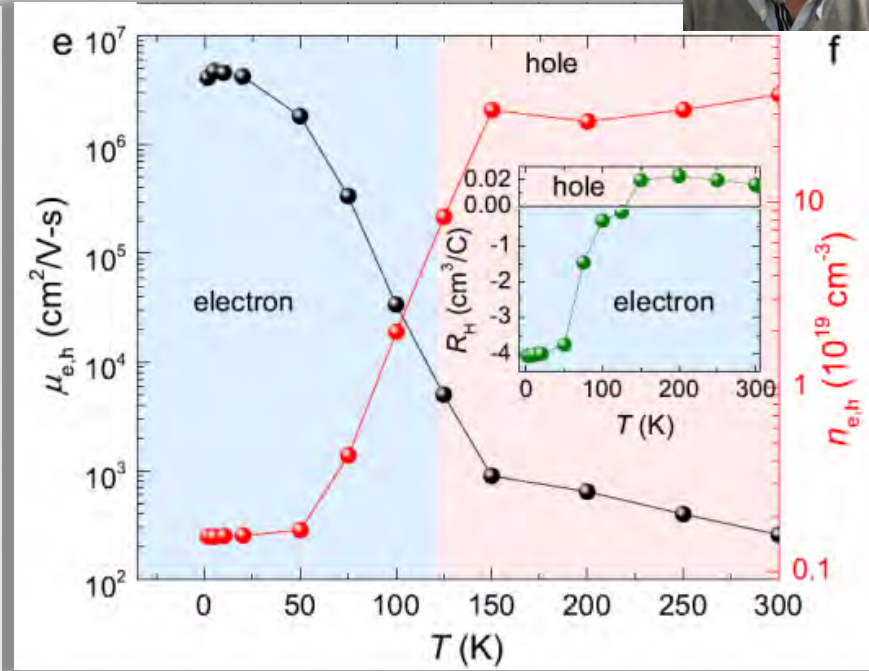
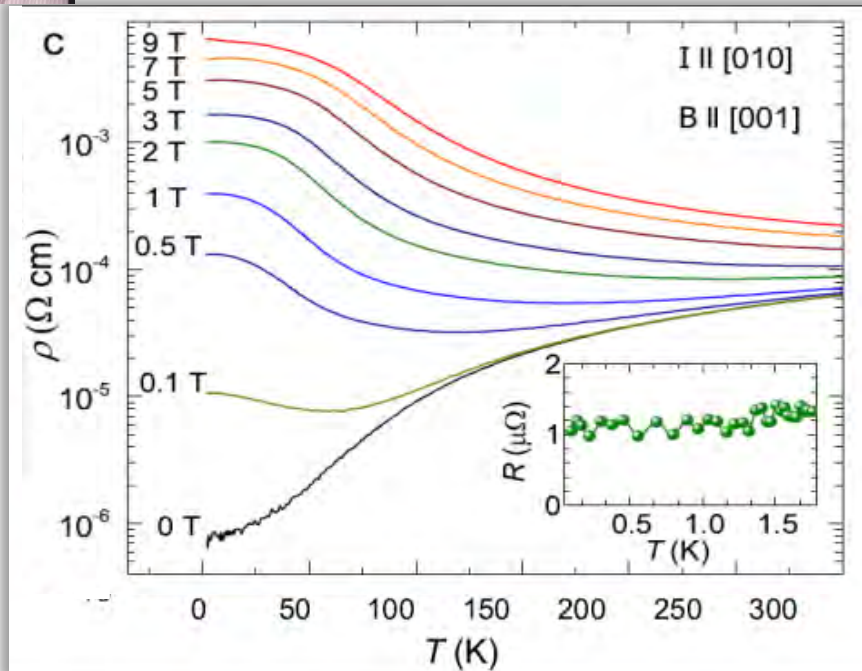
Increasing spin orbit coupling increases –
heavier elements
Distance between the Weyl points increases



Z. K. Liu et al., Nature Mat. 15 (2016) 27
Yang, et al. Nature Phys. 11 (2015) 728



Weyl semimetals in non-centro NbP

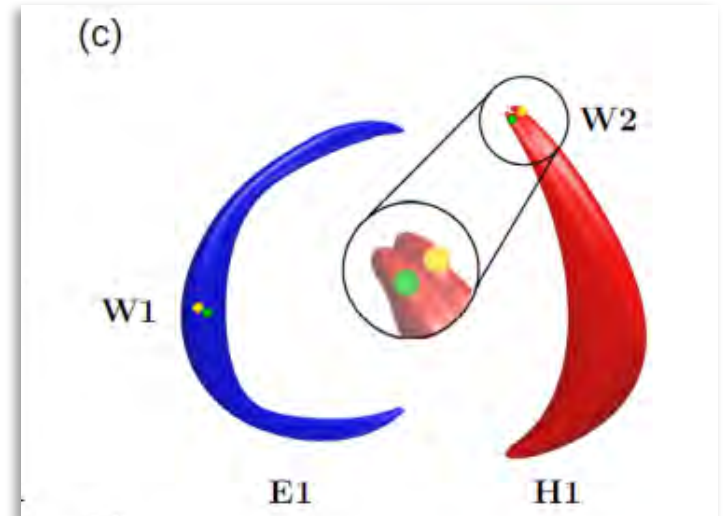
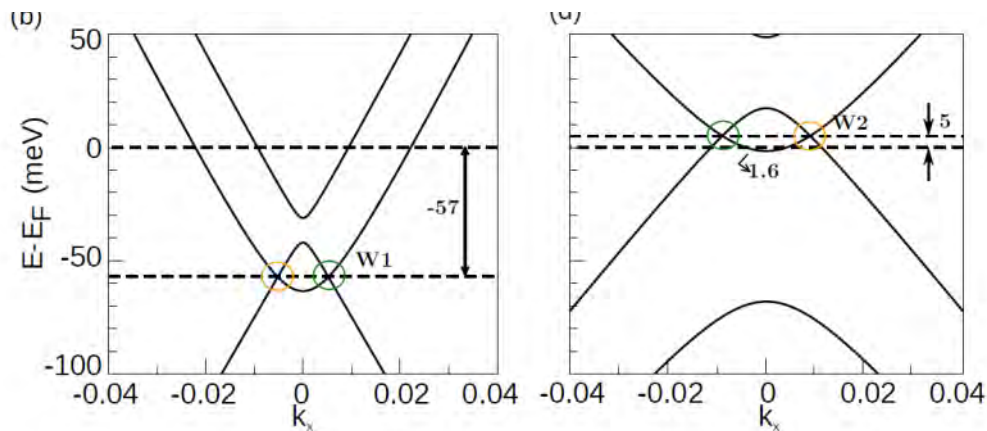
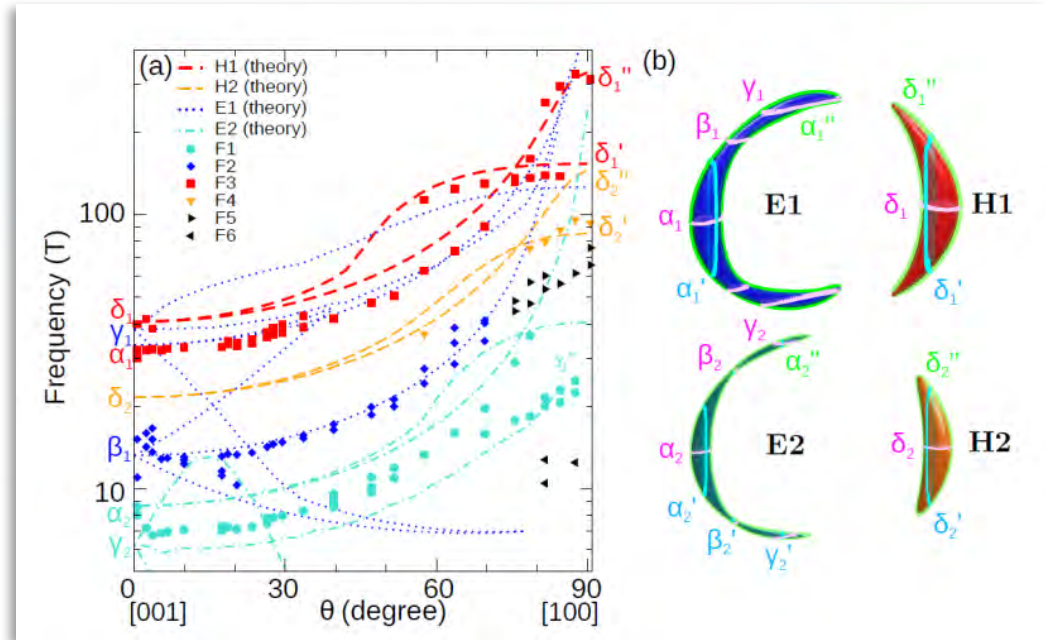
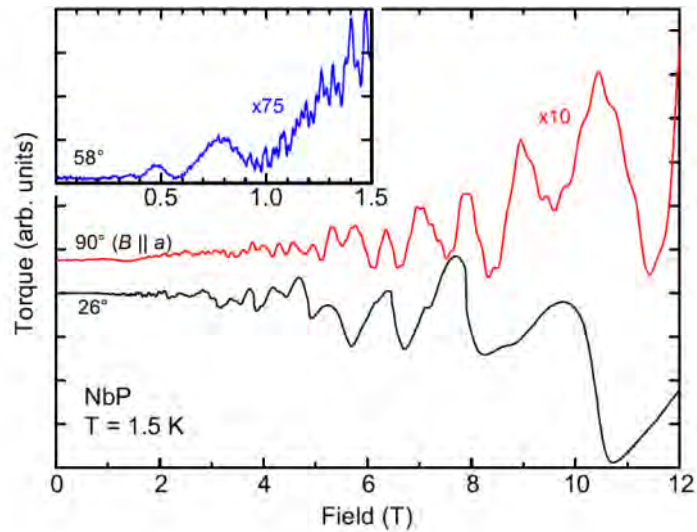


NbP is a topological Weyl semimetal

- with massless relativistic electrons
- extremely large magnetoresistance of **850,000%** at 1.85 K, 9T (250% at room temperature)
- an ultrahigh carrier mobility of **$5 \cdot 10^6 \text{ cm}^2 / \text{V s}$**

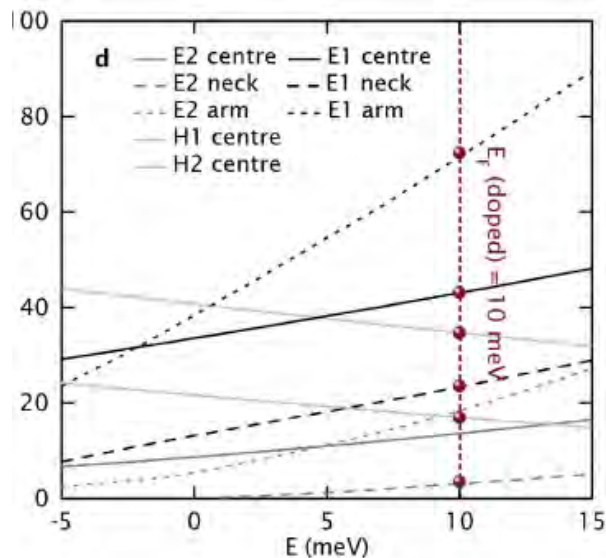
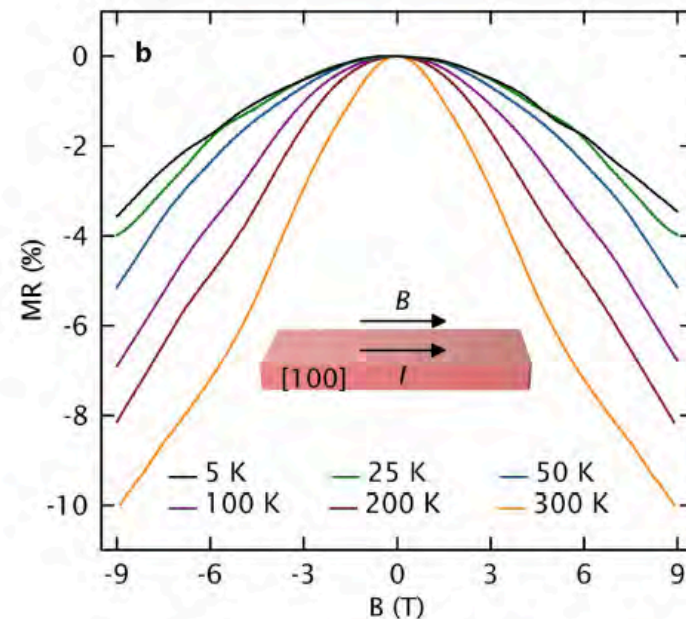
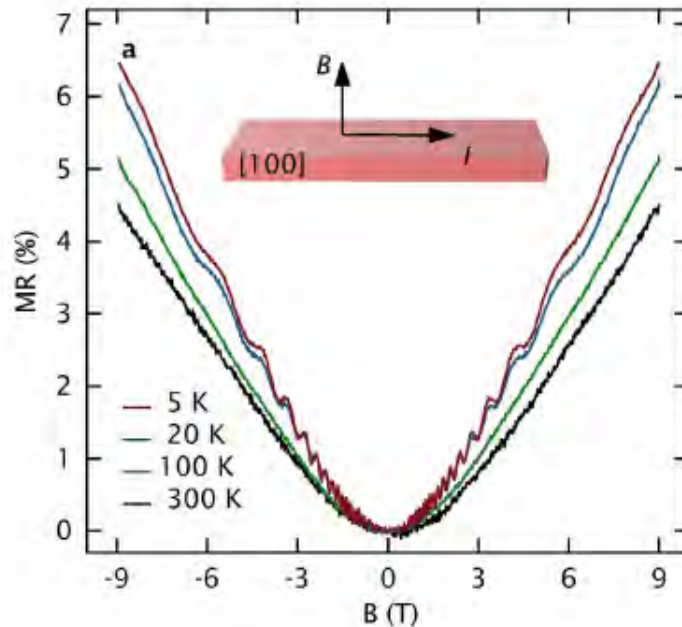


NbP and the Fermi surface





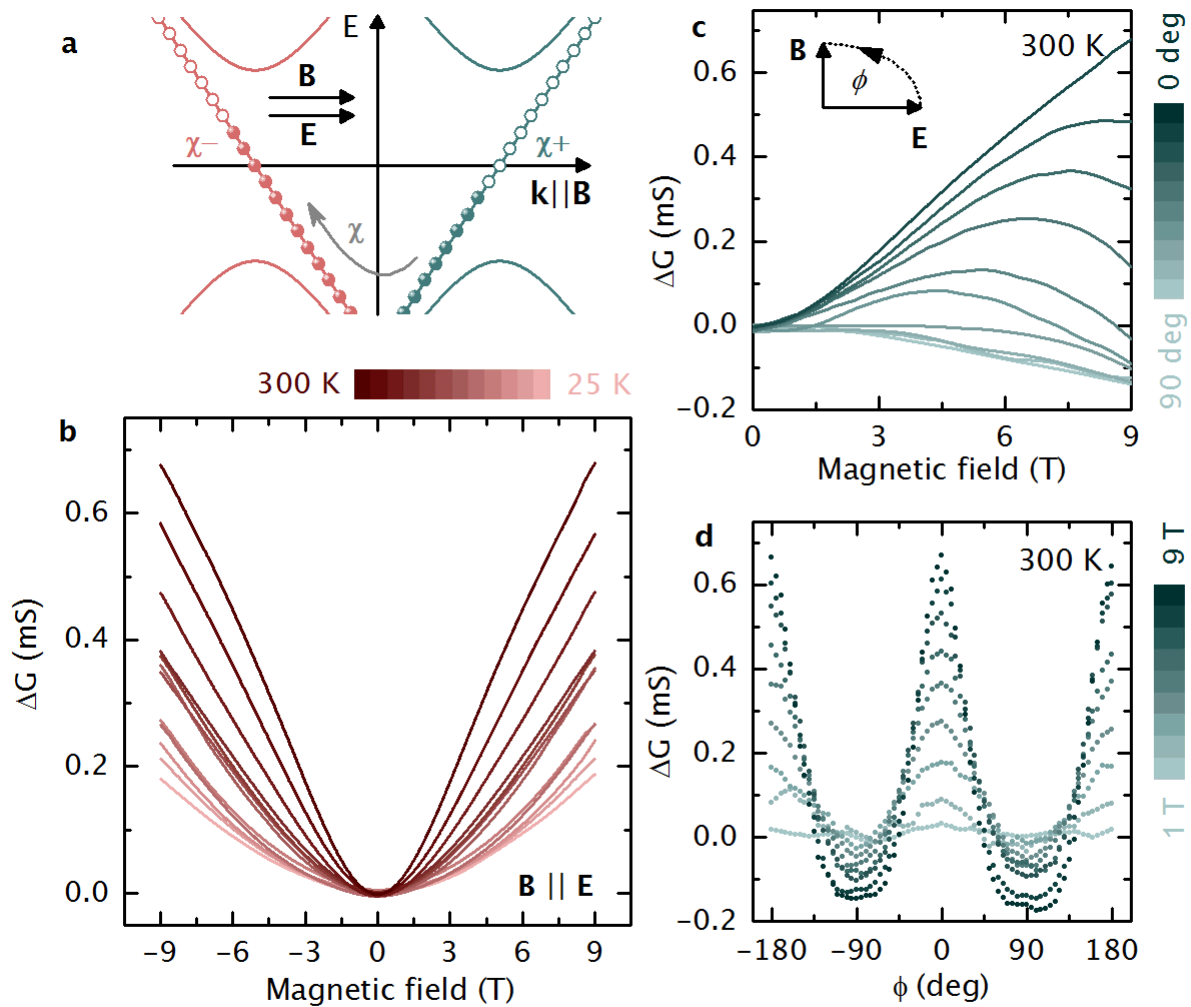
Chiral Anomaly



Ga-doping relocate the Fermi energy in NbP close to the W2 Weyl points
Therefore we observe a negative MR as a signature of the chiral anomaly the, NMR survives up to room temperature



Longitudinal magneto-transport – $E \parallel B$



The PMC is locked to $E \parallel B$, as expected for Chiral anomaly.



Chiral Anomaly

Experimental signatures for the mixed axial-gravitational anomaly in Weyl semimetals

- In solid state physics, mixed axial-gravitational anomaly can be identified by a positive magneto-thermoelectric conductance (PMTG) for $\Delta T \parallel B$.

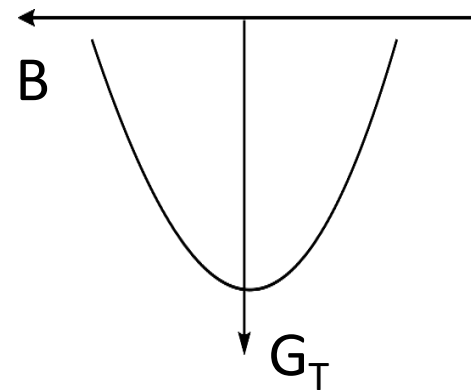
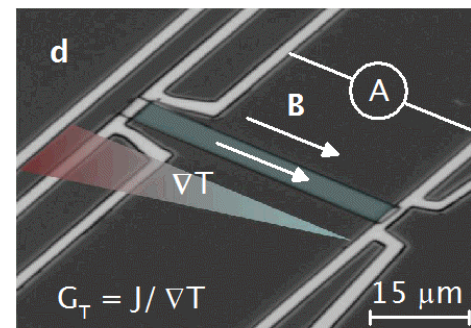
- Low fields: **quadratic**

$$G_T = d_{\text{th}} + c_2 a_\chi a_g B_{\parallel}^2$$

- High fields: **deminishes**

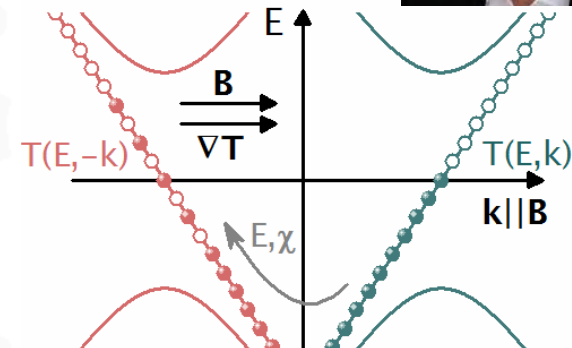
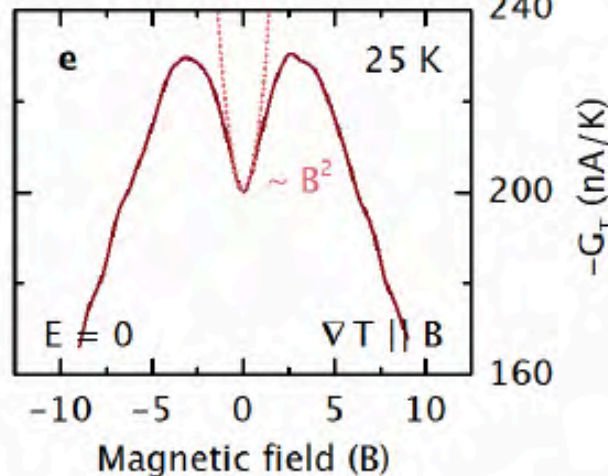
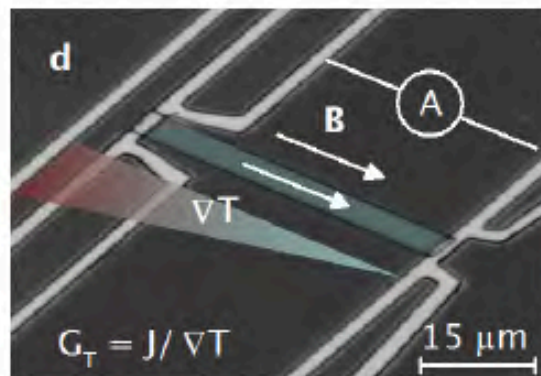
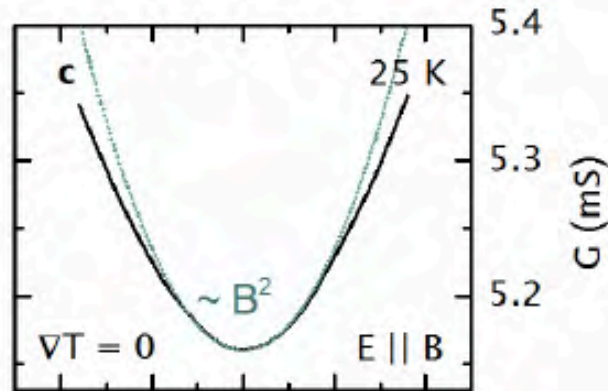
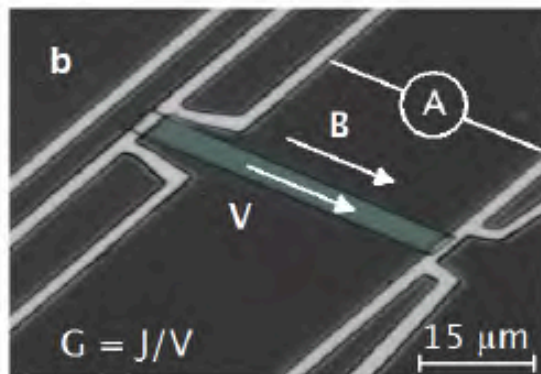
- $\Delta T \parallel B$ dictates sensitivity on alignment of B and ΔT .

\mathfrak{B}





Gravitational Anomaly

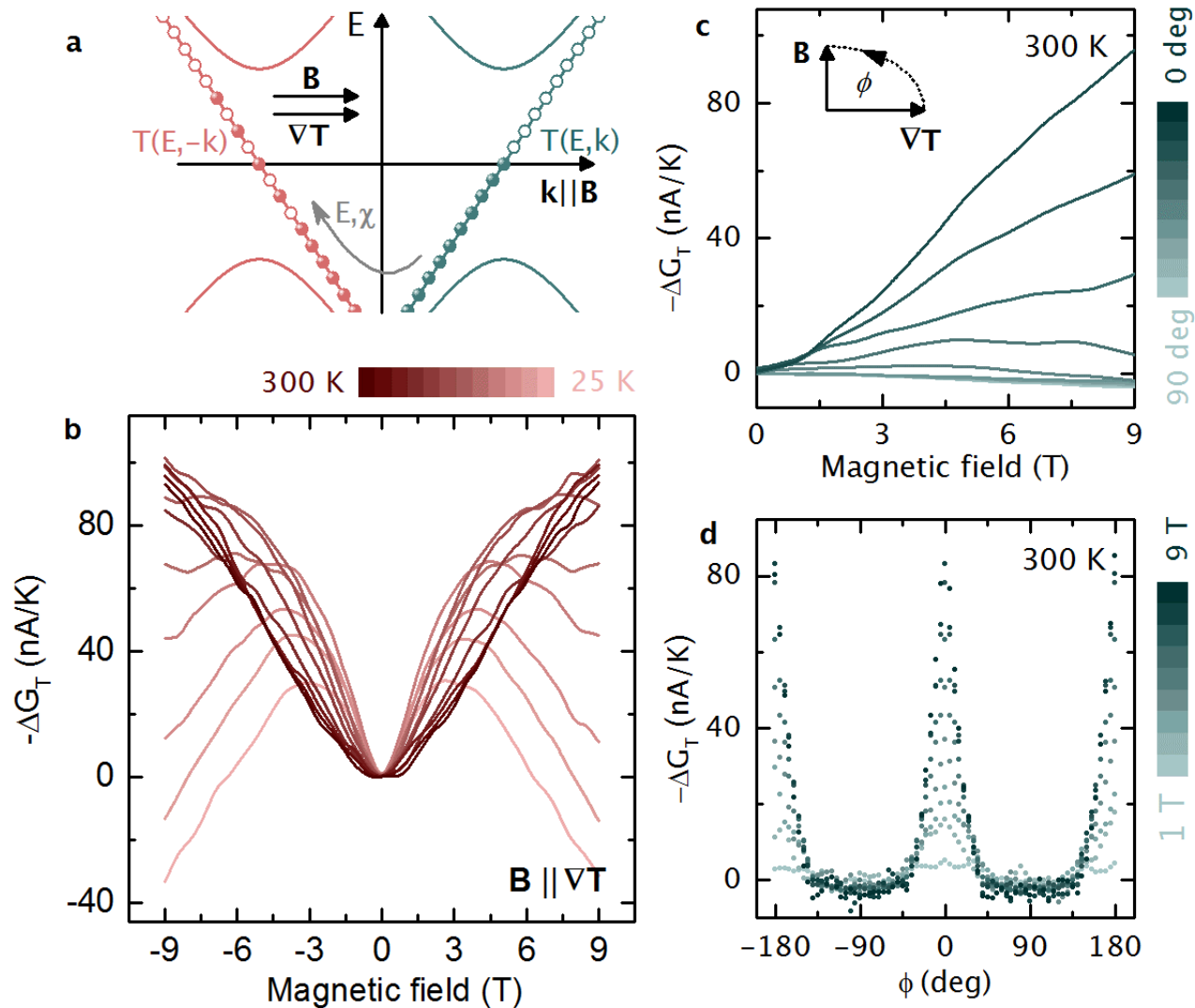


- Landsteiner, et al. Gravitational anomaly and transport phenomena. Phys. Rev. Lett. 107, 021601 (2011). URL
- Jensen, et al. Thermodynamics, gravitational anomalies and cones. Journal of High Energy Physics 2013, 88 (2013).
- Lucas, A., Davison, R. A. & Sachdev, S. Hydrodynamic theory of thermoelectric transport and negative magnetoresistance in weyl semimetals. PNAS 113, 9463–9468 (2016).

A positive longitudinal magneto-thermoelectric conductance (PMTC) in the Weyl semimetal NbP for collinear temperature gradients and magnetic fields that vanishes in the ultra quantum limit.



Longitudinal magneto-transport – $E \parallel B$



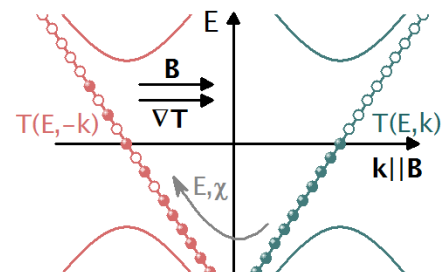
The PMTC is locked to $\Delta T \parallel B$, as expected for mixed-axial-gravitational anomaly.



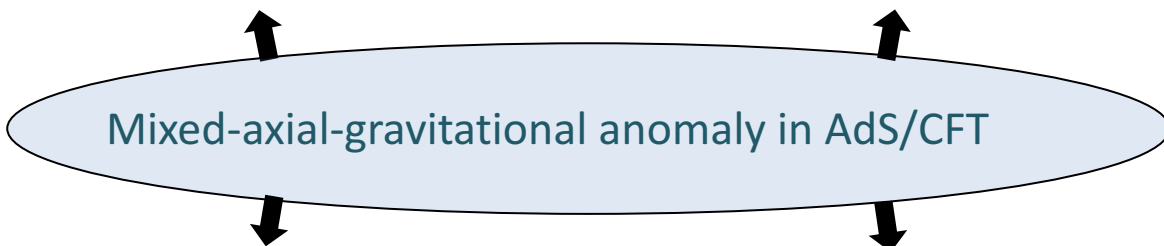
Axial-gravitational anomaly



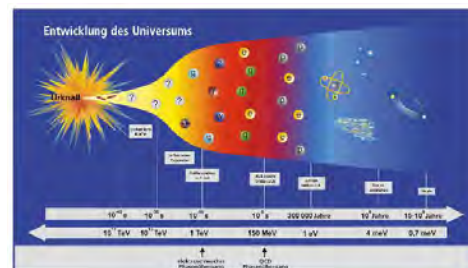
Neutron stars
(astronomy)



Positive MTG in Weyl semimetals
(solid state physics)



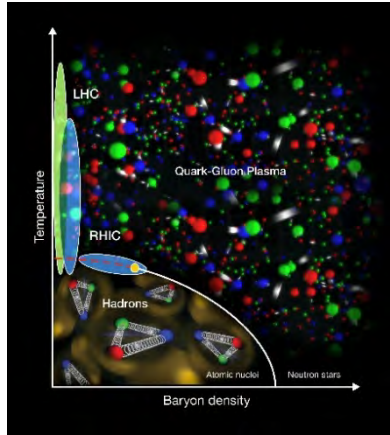
Pion decay



Baryogenesis in early universe
(cosmology)



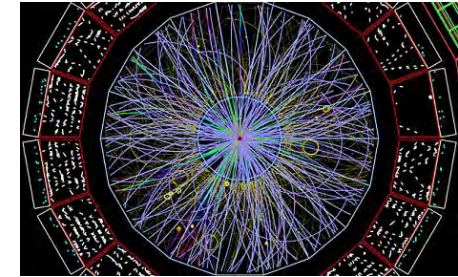
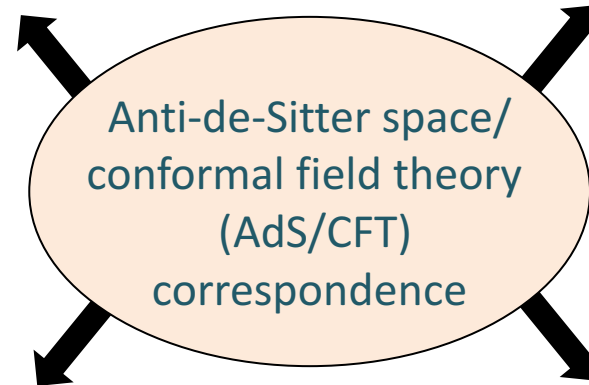
Holographic correspondence



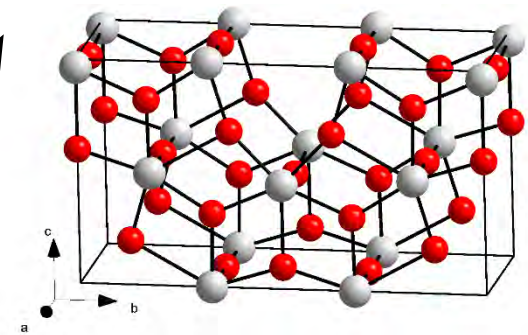
Baryogenesis
(cosmology)



Neutron stars
(astronomy)



Quark-gluon plasma
(colliders)



Condensed matter



Evidence for hydrodynamic electron flow in PdCoO₂

Philip J. W. Moll,^{1,2,3} Pallavi Kushwaha,³ Nabhanila Nandi,³ Burkhard Schmidt,³ Andrew P. Mackenzie^{3,4*}

Experimental evidence that the resistance of restricted channels of the ultra-pure two-dimensional metal PdCoO₂ has a large viscous contribution

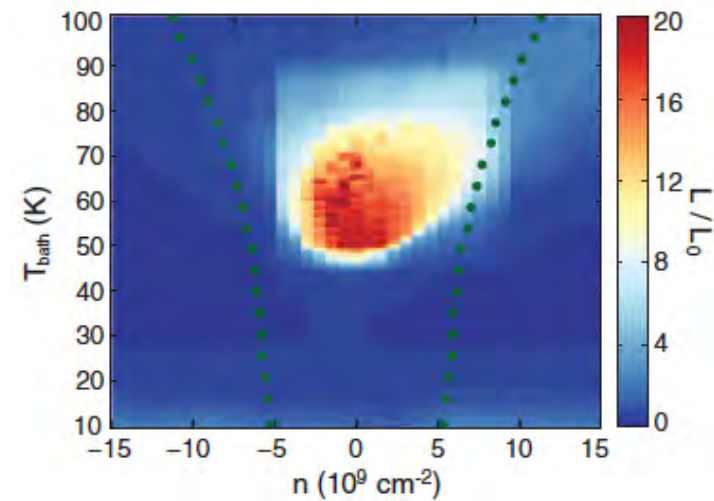
Negative local resistance caused by viscous electron backflow in graphene

D. A. Bandurin,¹ I. Torre,² R. Krishna Kumar,^{1,3} M. Ben Shalom,^{1,4} A. Tomadin,⁵ A. Principi,⁶ G. H. Auton,⁴ E. Khestanova,^{1,4} K. S. Novoselov,⁴ I. V. Grigorieva,¹ L. A. Ponomarenko,^{1,3} A. K. Geim,^{1*} M. Polini^{7*}

ELECTRON TRANSPORT

Observation of the Dirac fluid and the breakdown of the Wiedemann-Franz law in graphene

Jesse Crossno,^{1,2} Jing K. Shi,¹ Ke Wang,¹ Xiaomeng Liu,¹ Achim Harzheim,¹ Andrew Lucas,¹ Subir Sachdev,^{1,3} Philip Kim,^{1,2*} Takashi Taniguchi,⁴ Kenji Watanabe,⁴ Thomas A. Ohki,⁵ Kin Chung Fong^{5*}





Hydrodynamic electron flow in high-mobility wires

M. J. M. de Jong* and L. W. Molenkamp[†]

Philips Research Laboratories, 5656 AA Eindhoven, The Netherlands

(Received 24 October 1994)

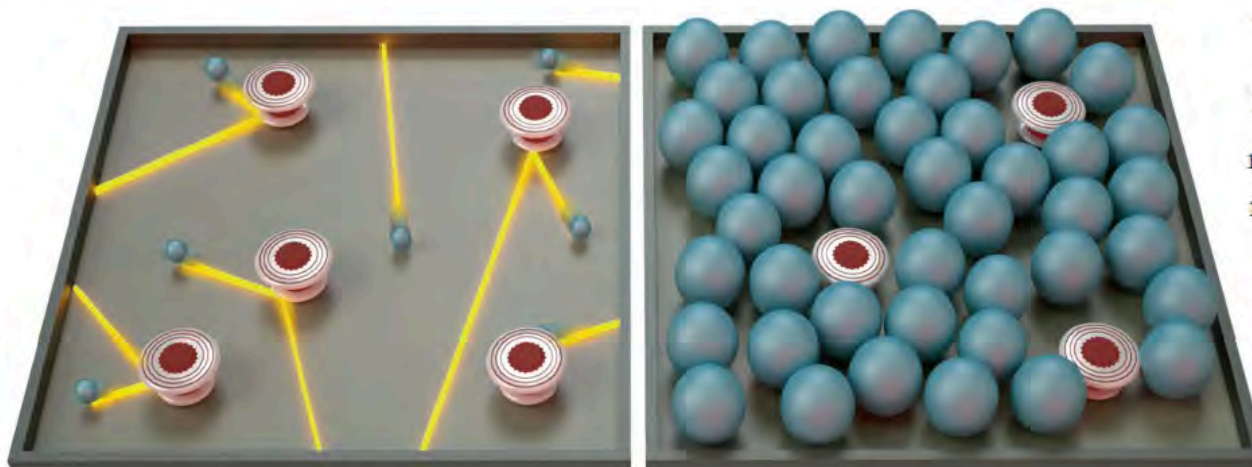
Hydrodynamic electron flow is experimentally observed in the differential resistance of electrostatically defined wires in the two-dimensional electron gas in (Al,Ga)As heterostructures. In these experiments current heating is used to induce a controlled increase in the number of electron-electron collisions in the wire. The interplay between the partly diffusive wire-boundary scattering and the electron-electron scattering leads first to an increase and then to a decrease of the resistance of the wire with increasing current. These effects are the electronic analog of Knudsen and Poiseuille flow in gas transport, respectively. The electron flow is studied theoretically through a Boltzmann transport equation, which includes impurity, electron-electron, and boundary scattering. A solution is obtained for arbitrary scattering parameters. By calculation of flow profiles inside the wire it is demonstrated how normal flow evolves into Poiseuille flow. The boundary-scattering parameters for the gate-defined wires can be deduced from the magnitude of the Knudsen effect. Good agreement between experiment and theory is obtained.



PHYSICS

Electrons go with the flow in exotic material systems

Electronic hydrodynamic flow—making electrons flow like a fluid—has been observed



- Hydrodynamic electron fluid is defined by momentum-conserving electron-electron scattering
- Violation of Wiedeman-Franz law
- Viscosity-induced shear forces making the electrical resistivity a function of the channel width

REFERENCES

1. J. Crossno, J. K. Shi, K. Wang, X. Liu, A. Harzheim, A. Lucas, S. Sachdev, P. Kim, T. Taniguchi, K. Watanabe, T. A. Ohki, K. C. Fong, *Science* **351**, 1058 (2016).
2. D. A. Bandurin, I. Torre, R. Krishna Kumar, M. Ben Shalom, A. Tomadin, A. Principi, G. H. Auton, E. Khestanova, K. S. Novoselov, I. V. Grigorieva, L. A. Ponomarenko, A. K. Geim, M. Polini, *Science* **351**, 1055 (2016).
3. P. J. W. Moll *et al.*, *Science* **351**, 1061 (2016).
4. J. Zaanen, Y.-W. Sun, Y. Liu, K. Schalm, *Holographic Duality in Condensed Matter Physics* (Cambridge Univ. Press, 2015).
5. S. A. Hartnoll, P. K. Kovtun, M. Mueller, S. Sachdev, *Phys. Rev. B* **76**, 144502 (2007).
6. A. H. Castro Neto *et al.*, *Rev. Mod. Phys.* **81**, 109 (2009).
7. M. Mueller, J. Schmalian, L. Fritz, *Phys. Rev. Lett.* **103**, 025301 (2009).
8. M. S. Foster, I. L. Aleiner, *Phys. Rev. B* **79**, 085415 (2009).
9. A. Lucas, J. Crossno, K. C. Fong, P. Kim, S. Sachdev, <http://arxiv.org/abs/1510.01738> (2015).
10. L. Levitov, G. Falkovich, <http://arxiv.org/abs/1508.00836> (2015).
11. M. J. M. de Jong, L. W. Molenkamp, *Phys. Rev. B* **51**, 13389 (1995).



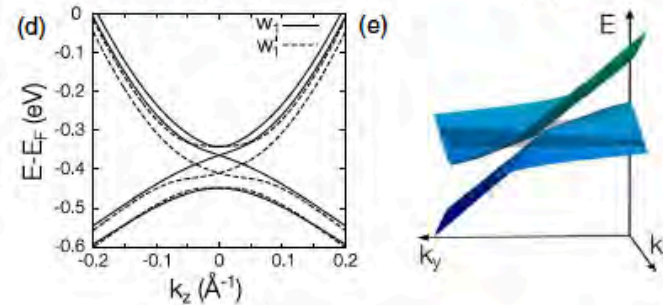
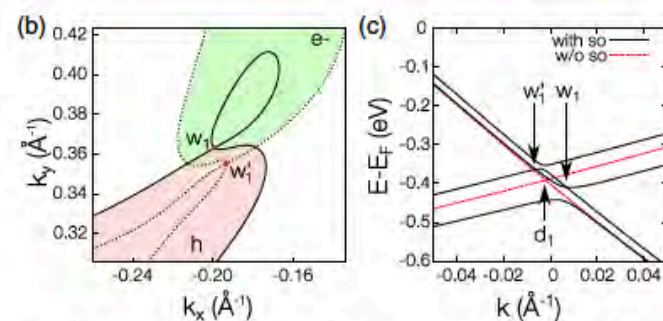
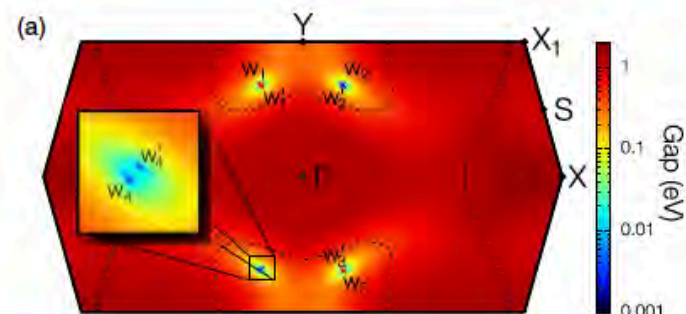
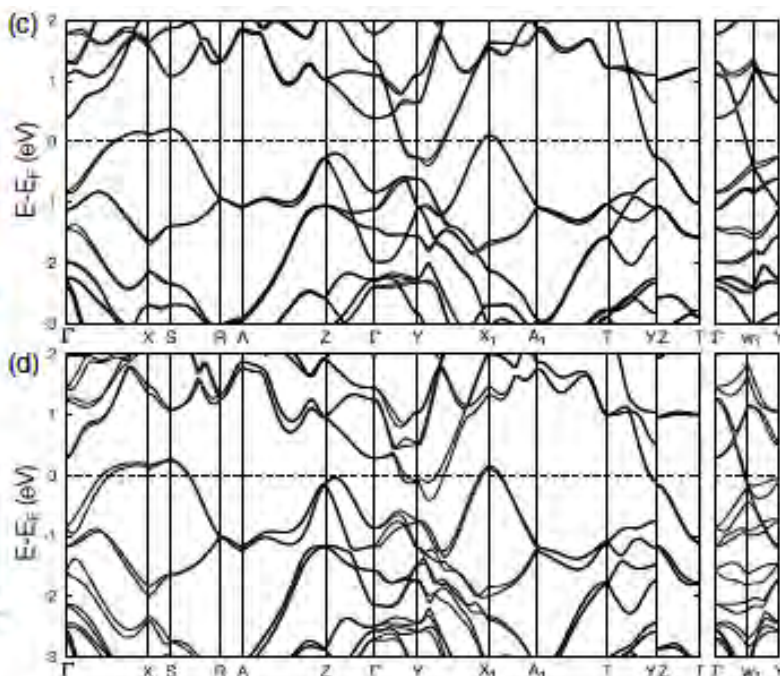
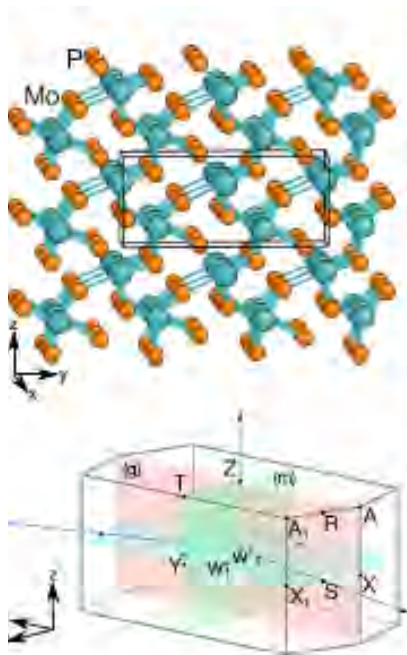
Weyl Semimetals

WP2



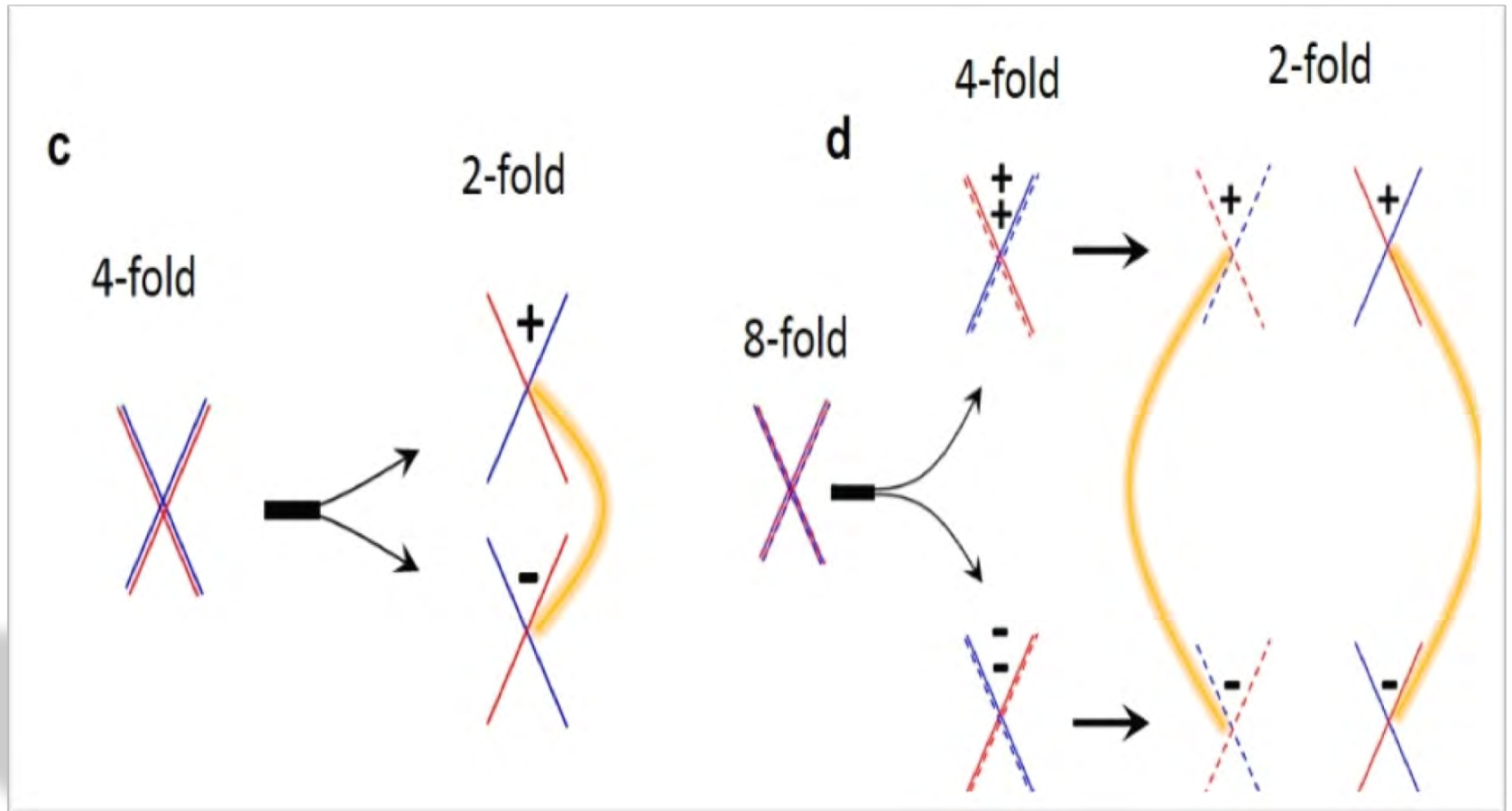
Robust Type-II Weyl Semimetal Phase in Transition Metal Diphosphides XP₂ (X = Mo, W)

G. Autès,^{1,2} D. Gresch,³ M. Troyer,³ A. A. Soluyanov,^{3,4} and O. V. Yazyev^{1,2}



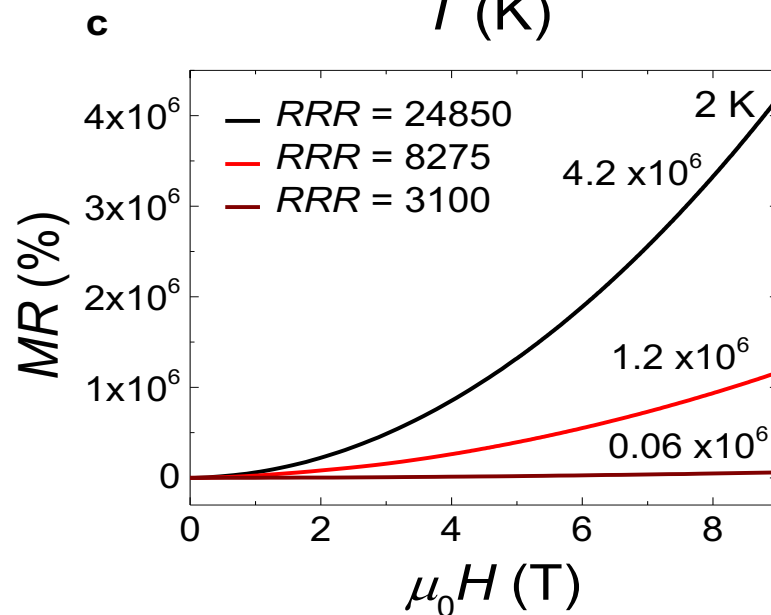
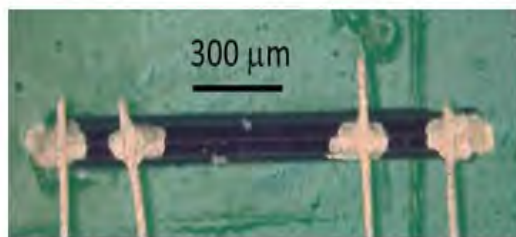
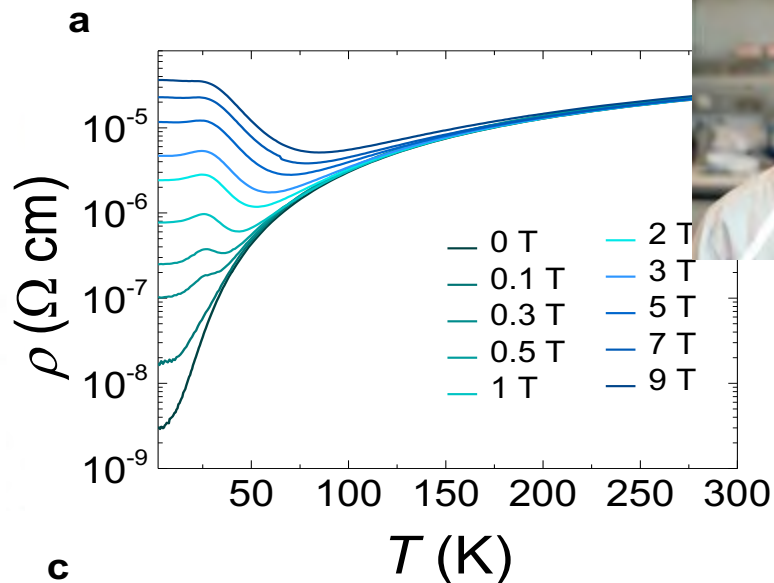
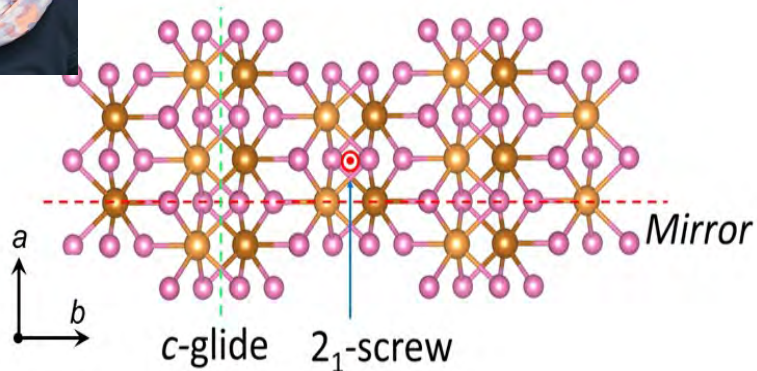


WP₂ protected Weyl



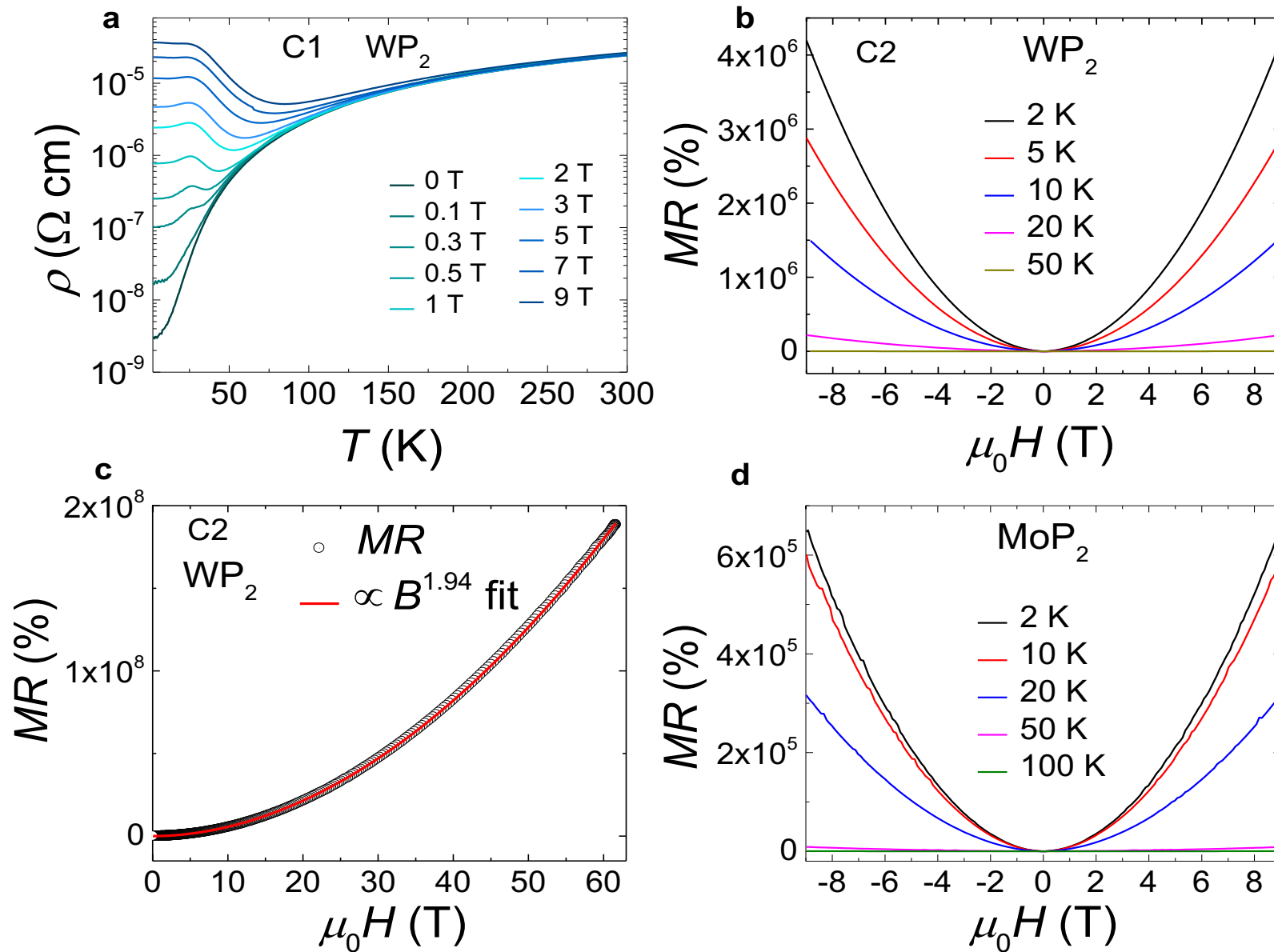


WP₂ protected Weyl



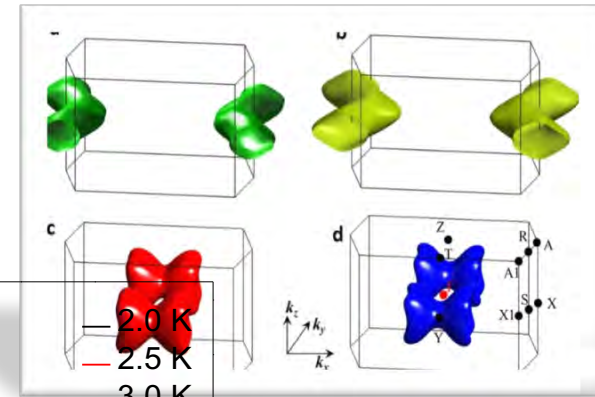
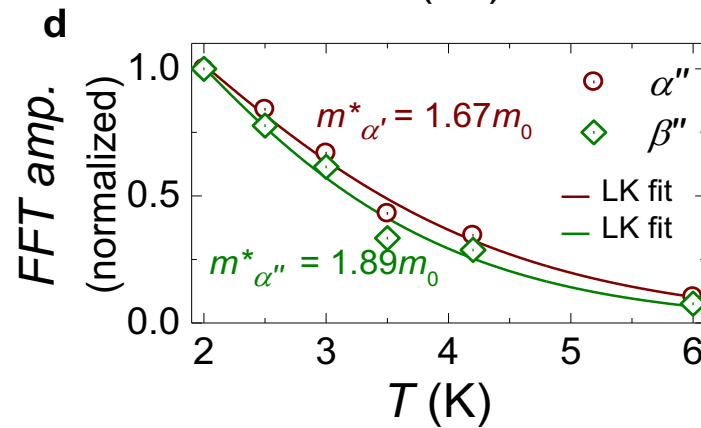
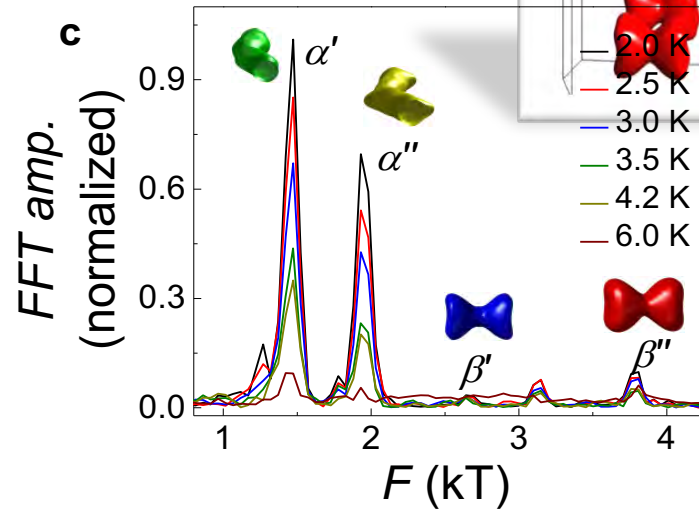
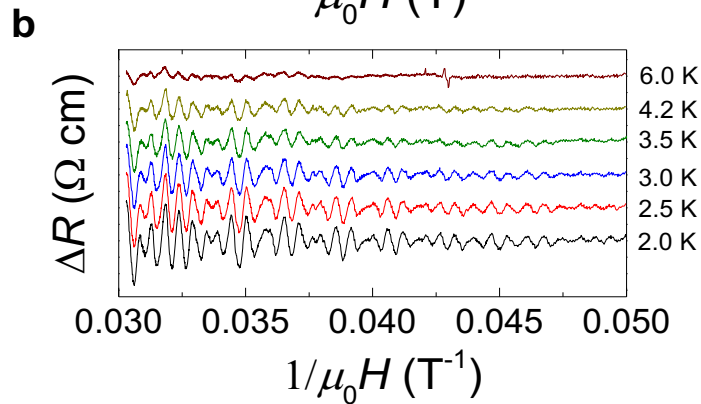
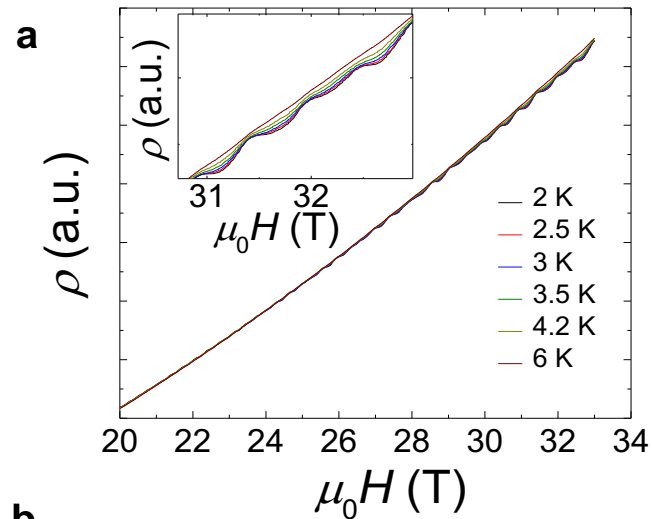


MoP₂ and WP₂



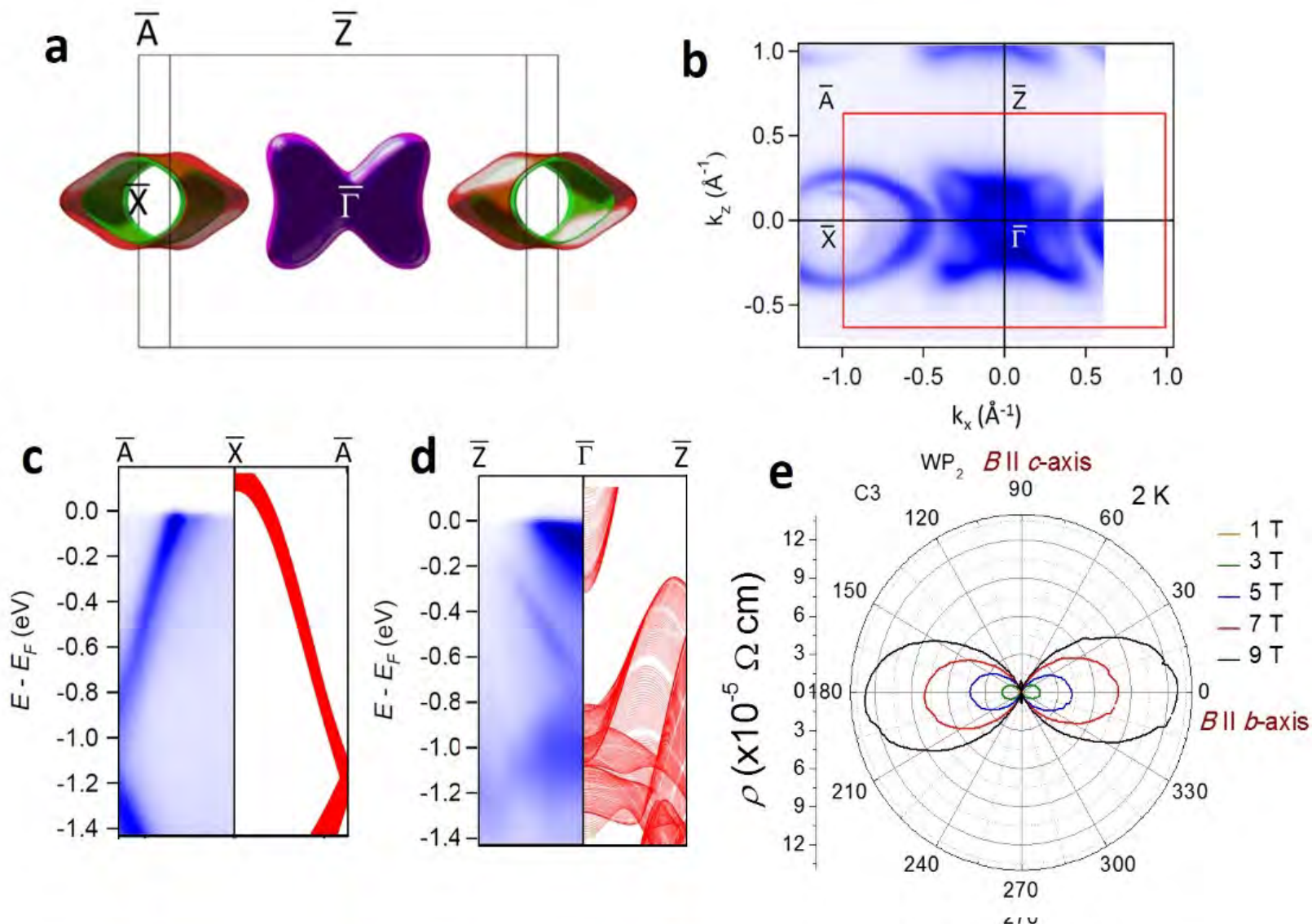


WP₂ protected Weyl





ARPES and the band structure



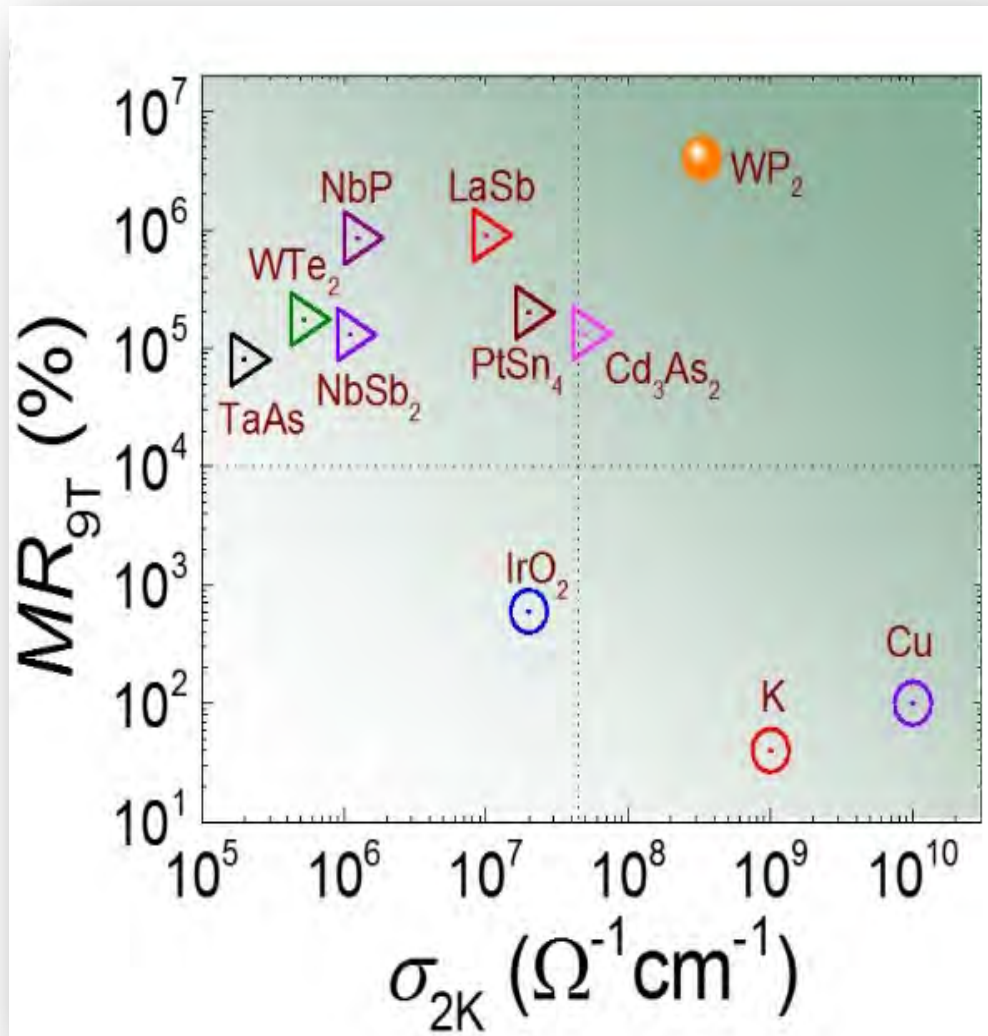
Photoemission, Nan Xu, Ming Shi, Paul Scherrer Institute, Swiss Light Source, CH-5232 Villigen PSI, Switzerland.

Extremely high magnetoresistance and conductivity in the type-II Weyl semimetal WP₂, Nitesh, et al.; arXiv:1703.04527



WP₂ protected Weyl

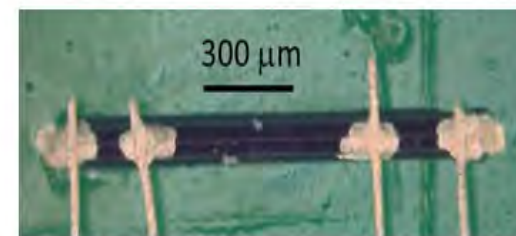
Magnetotransport in a novel Weyl WP₂





Macroscopic mean free path

Compound	ρ (Ωcm)	l (μm)	μ ($\text{cm}^2\text{V}^{-1}\text{s}^{-1}$)	n (cm^{-3})
MoP	6×10^{-9}	11	2.4×10^4	2.9×10^{22}
WP ₂	3×10^{-9}	530	4×10^6	5×10^{20}
WC	0.35×10^{-6}		$\sim 1 \times 10^4$	4×10^{20}
PtCoO ₂	40×10^{-9}	5	0.7×10^4	2.2×10^{22}
PdCoO ₂	9×10^{-9}	20	2.8×10^4	2.4×10^{22}



WC J. B. He et al. arXiv:1703.03211

Pallavi Kushwaha, et al. Sci. Adv.1 (2015) e150069

P. Moll Science 351, (2016) 1061

Chandra Shekhar et al. arXiv:1703.03736

Nitesh, et al.; arXiv:1703.04527



Hydrodynamic Electron Flow and Hall Viscosity

Thomas Scaffidi,¹ Nabhanila Nandi,² Burkhard Schmidt,² Andrew P. Mackenzie,^{2,3} and Joel E. Moore^{1,4}

In the ballistic regime ($w \ll l_{\text{er}}, l_{\text{mr}}$): $\rho \sim w^{-1}$

Hydrodynamic effects become dominant

- electron-electron scattering $l_{\text{er}} \ll w \ll l_{\text{mr}}$
- with electron-electron scattering length $l_{\text{er}} = v_{\text{F}}\tau_{\text{er}}$
- w the sample width,
- $l_{\text{mr}} = v_{\text{F}}\tau_{\text{mr}}$ the mean free path and v_{F} the Fermi velocity

In the Navier-Stokes flow limit: $\rho = m^*/(e^2n) \cdot 12\eta w^{-2}$

R. N. Gurzhy, A. N. Kalinenko, A. I. Kopeliovich, Hydrodynamic effects in the electrical conductivity of impure metals. *Sov. Physics-JETP*. **69**, 863–870 (1989).

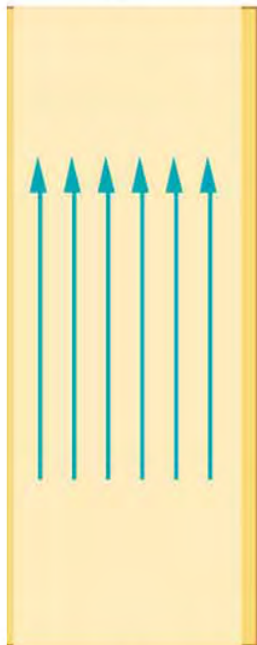
P. S. Alekseev, Negative magnetoresistance in viscous flow of two-dimensional electrons. *Phys. Rev. Lett.* **117** (2016).

T. Scaffidi, N. Nandi, B. Schmidt, A. P. Mackenzie, J. E. Moore, Hydrodynamic Electron Flow and Hall Viscosity. *Phys. Rev. Lett.* **118**, 226601 (2017).

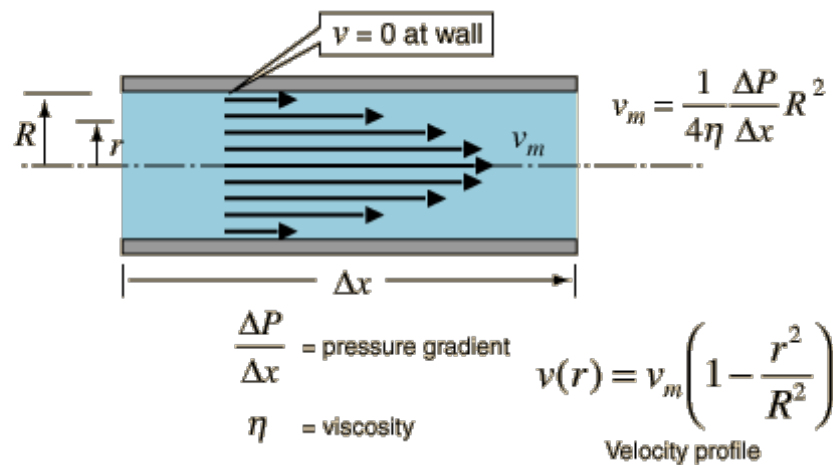
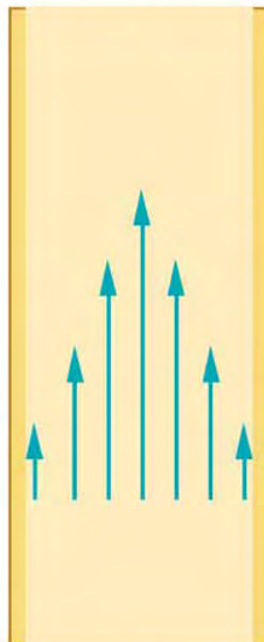


Water, Gas or Electrons

Nonviscous
 $\eta = 0$

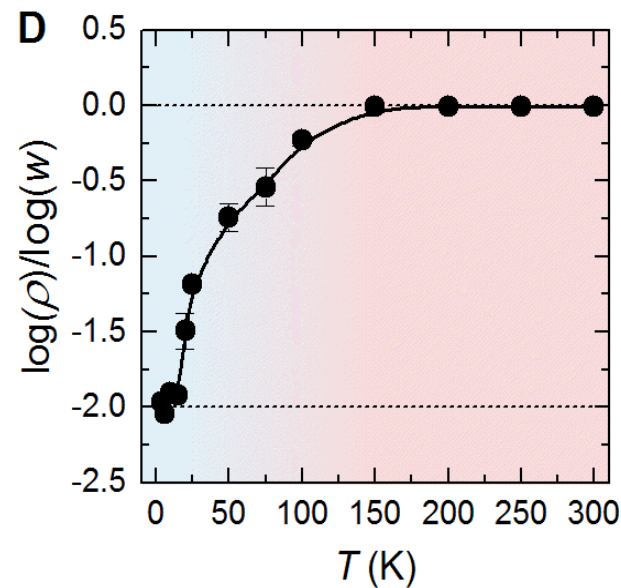
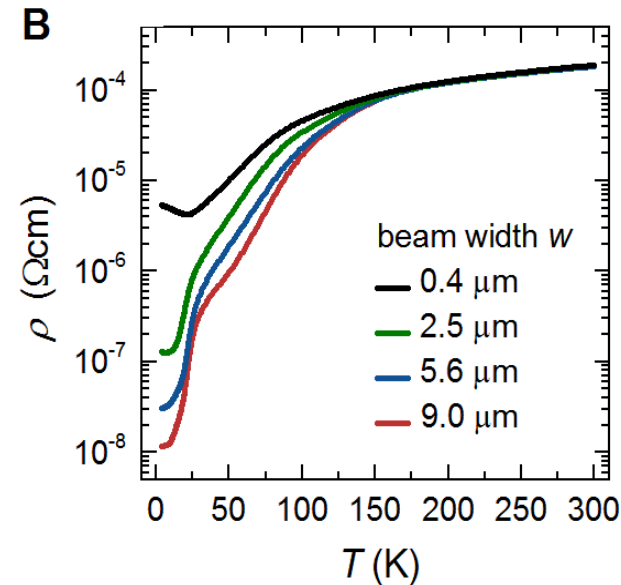
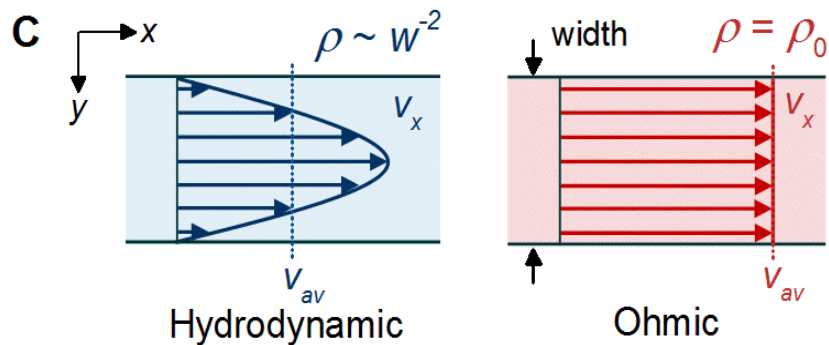
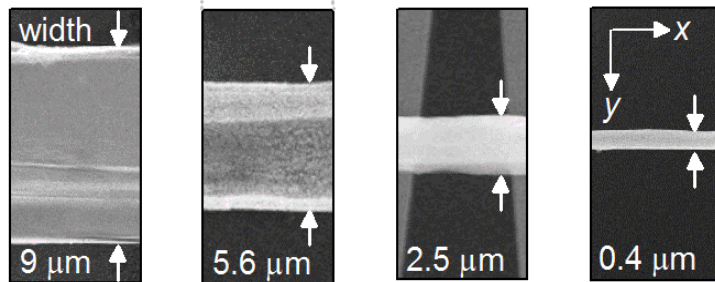
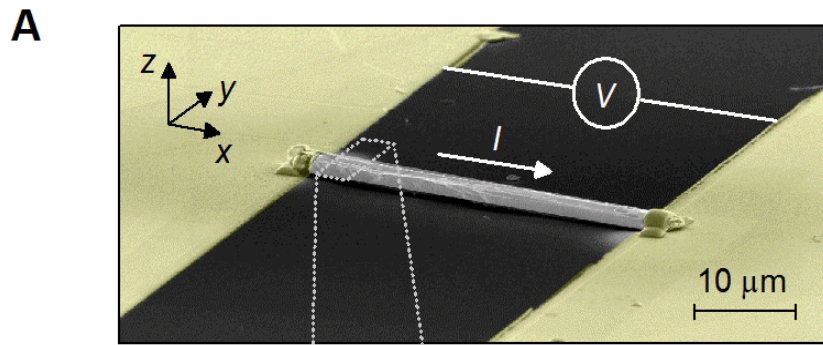


Viscous



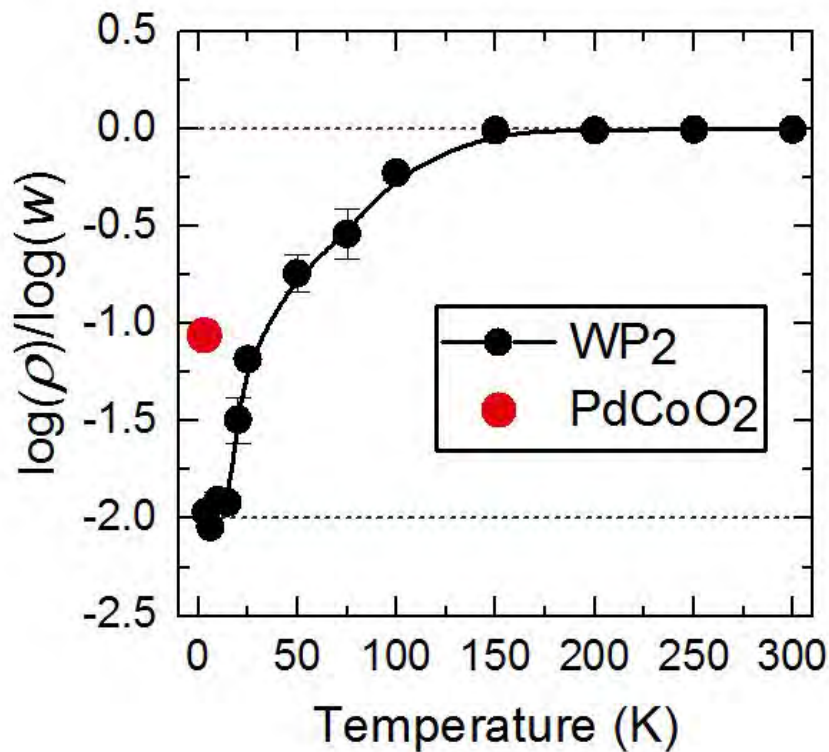
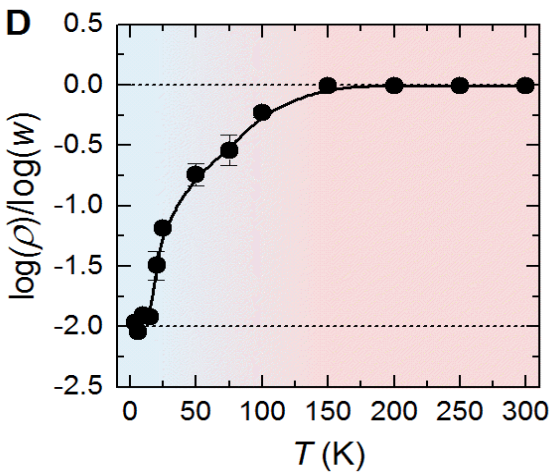
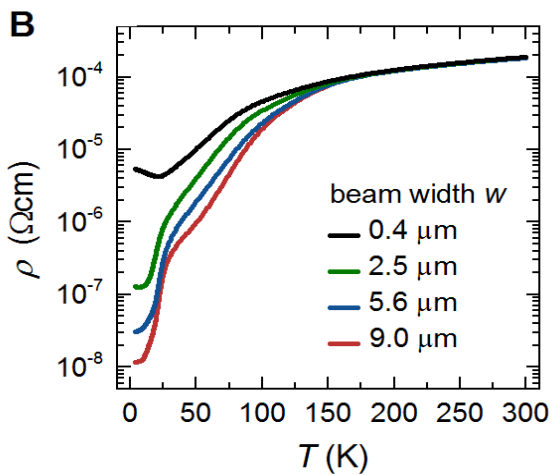
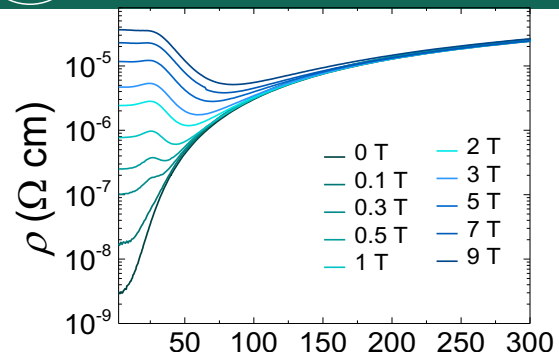


Hydrodynamic flow





Hydrodynamic flow

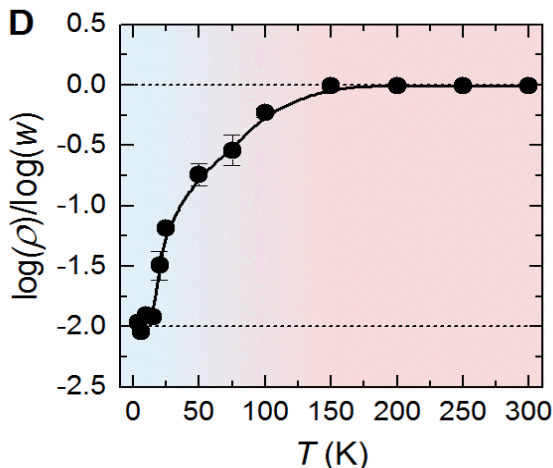
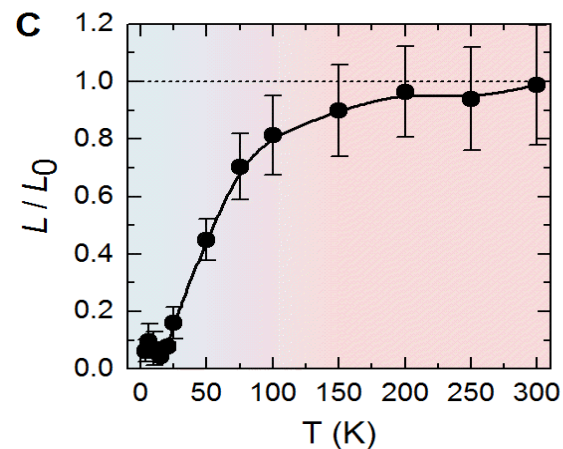
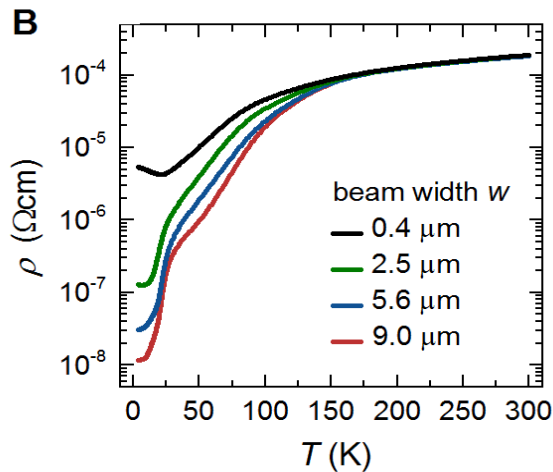
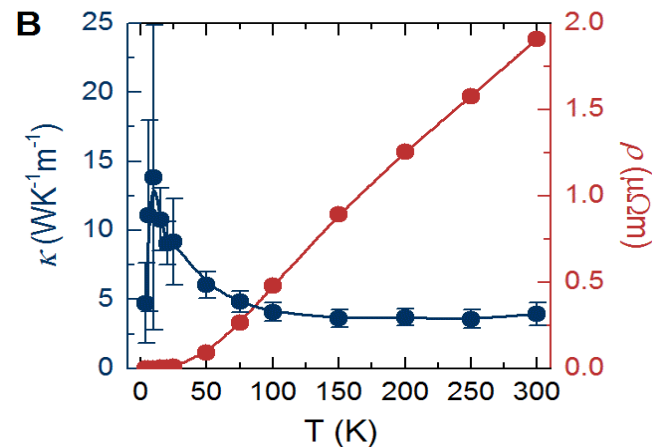
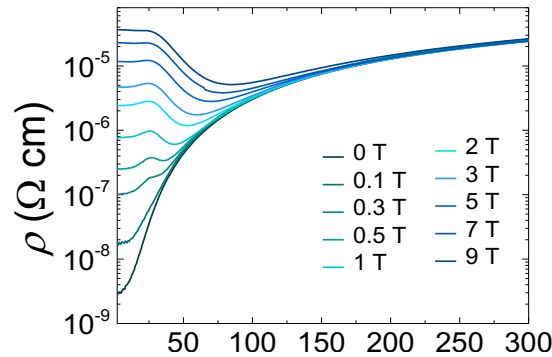
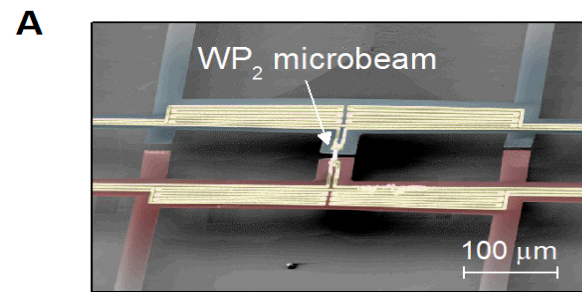


P. J. W. Moll *et al.*, *Science* 10.1126/science.aac8385 (2016).

J. Gooth *et al.* submitted, arXiv:1706.05925



Hydrodynamic flow



- Hydrodynamic electron fluid <15K
- conventional metallic state at T higher 150K

The hydrodynamic regime:

- a viscosity-induced dependence of the electrical resistivity on the square of the channel width
- But independent of the thermal conductivity

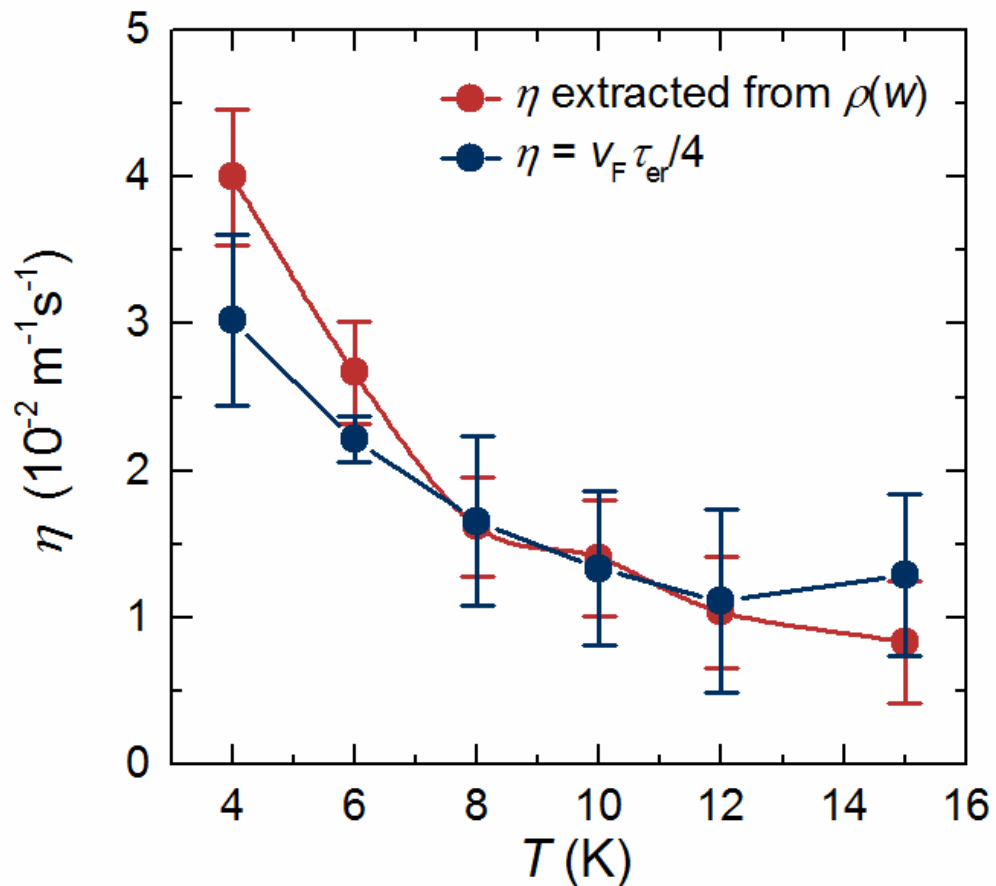
$$\rho = m^*/(e^2 n) \cdot 12 \eta w^{-2}$$

- a strong violation of the Wiedemann-Franz law

$$L \equiv \frac{\kappa}{\sigma T} = \frac{\pi^2}{3} \equiv L_0$$



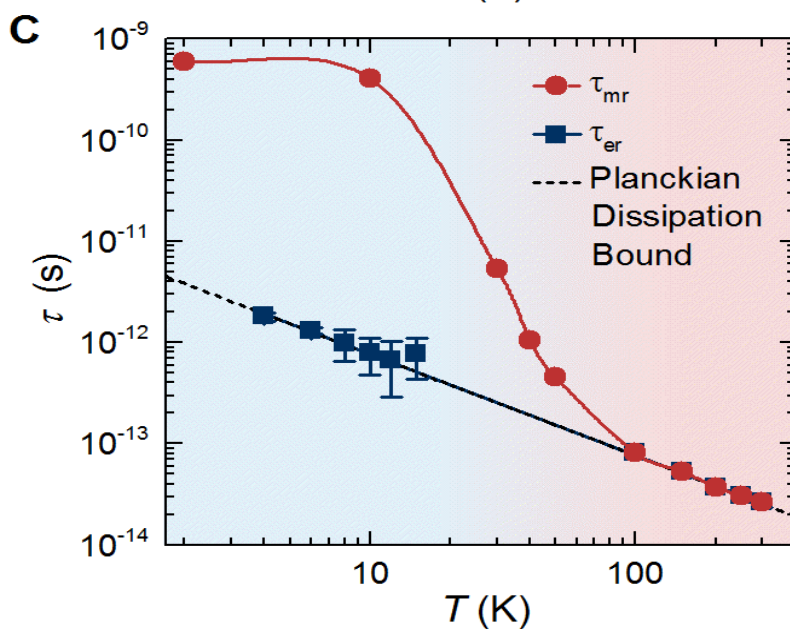
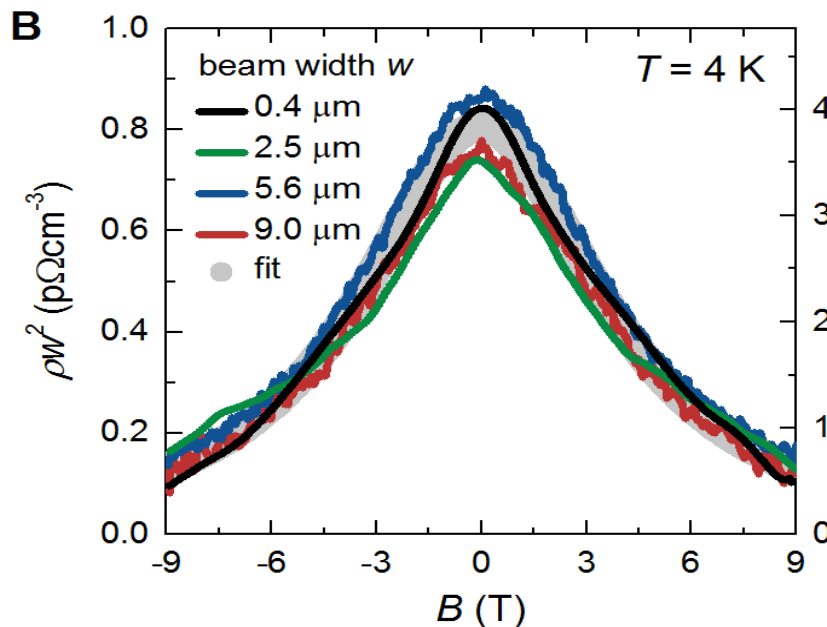
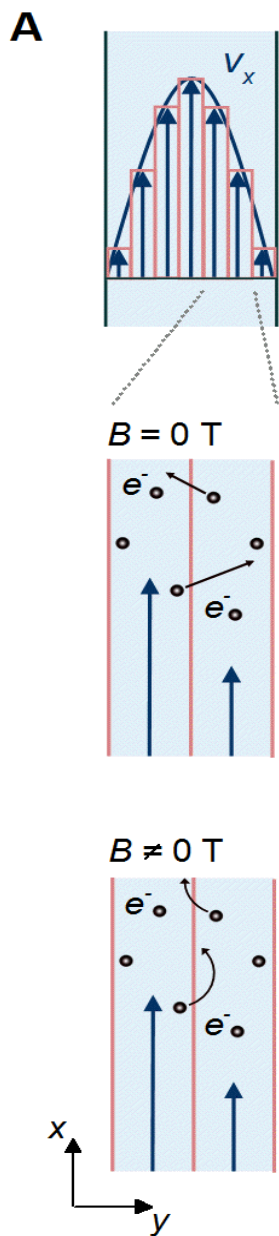
Viscosity of the electron fluid in WP₂



The dynamic viscosity is $\eta_D = 1 \times 10^{-4} \text{ kg m}^{-1} \text{ s}^{-1}$ at 4 K.



Magnetohydrodynamics, Planckian bound of dissipation



Grey dots: the magneto-hydrodynamic model in the Navier-Stokes flow limit

Momentum relaxation times t_{mr}

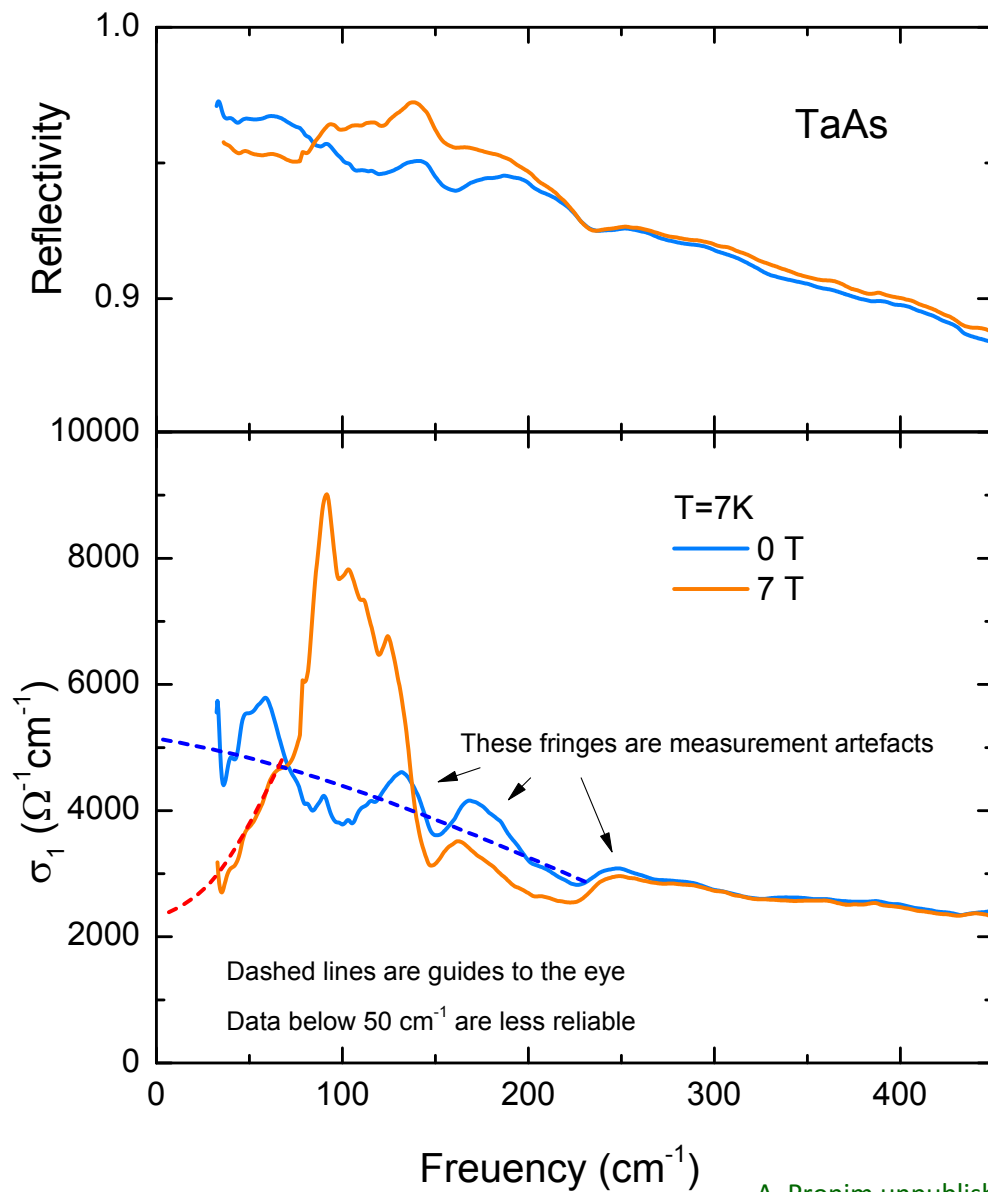
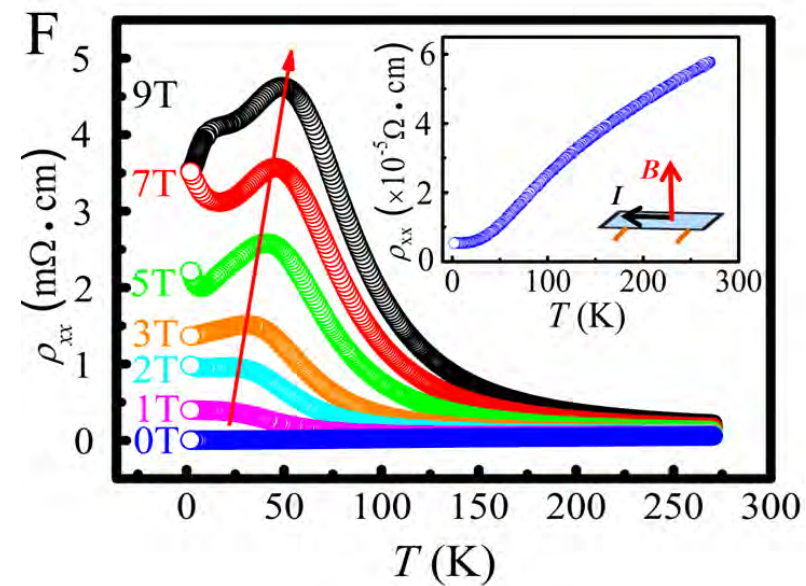
Thermal energy relaxation times t_{er}

Dashed line marks the Planckian bound on the dissipation time $\tau_{\hbar} = \hbar/(k_B T)$.

Both times saturate the bound posed by the uncertainty principle at all temperatures



TaAs

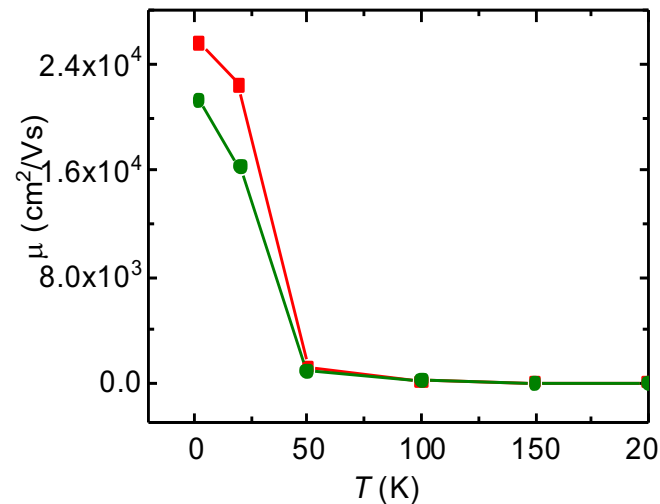
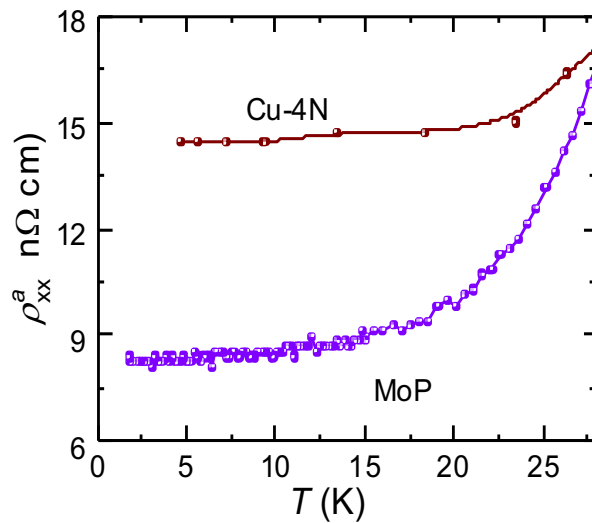
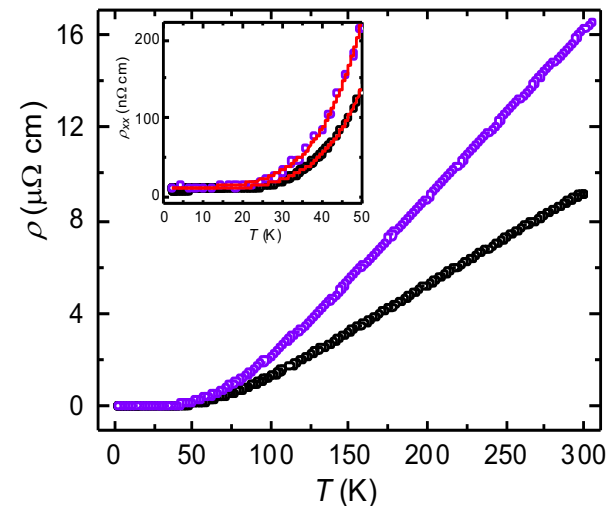
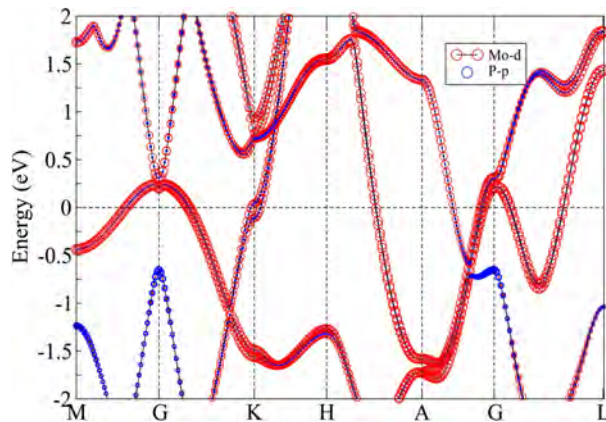
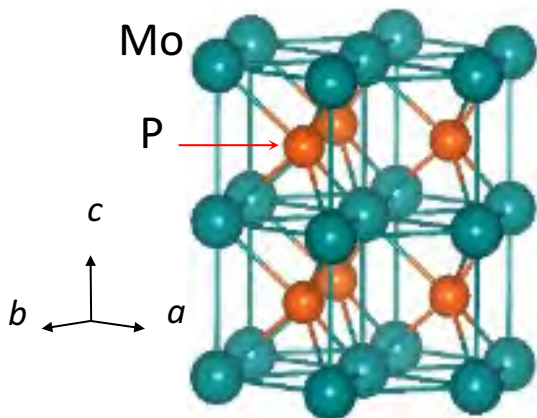




Topological Metals



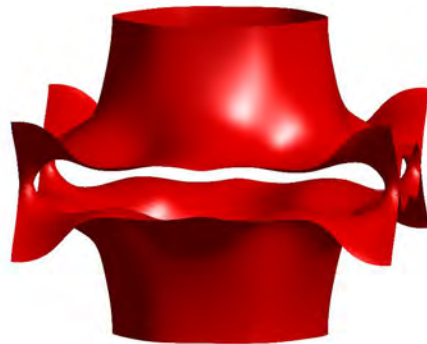
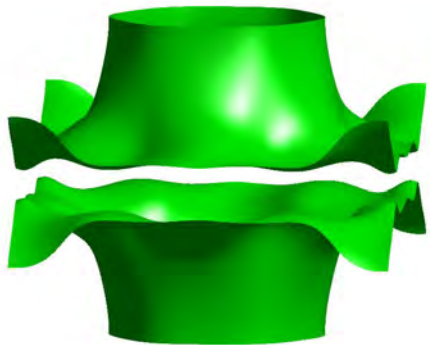
MoP better than Copper



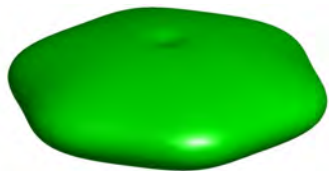
3D-Hydrodynamics ?



Fermi surfaces



$$2.7 \times 10^{22} \text{ cm}^{-3}$$



$$1.12 \times 10^{21} \text{ cm}^{-3}$$



$$2.57 \times 10^{20} \text{ cm}^{-3}$$



Experimental measurement is around

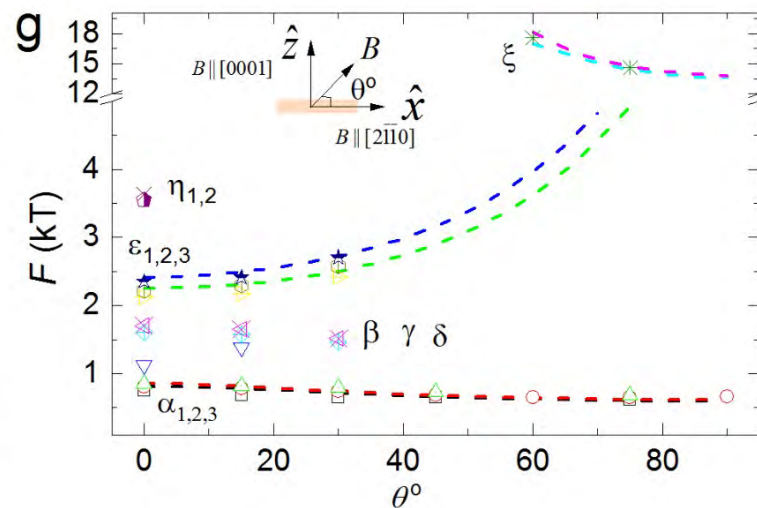
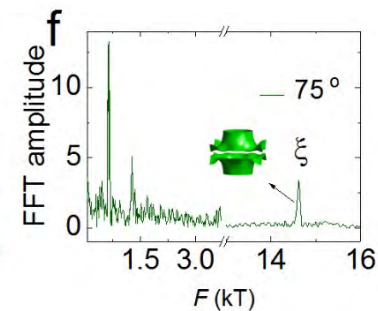
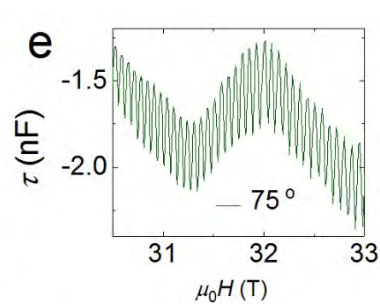
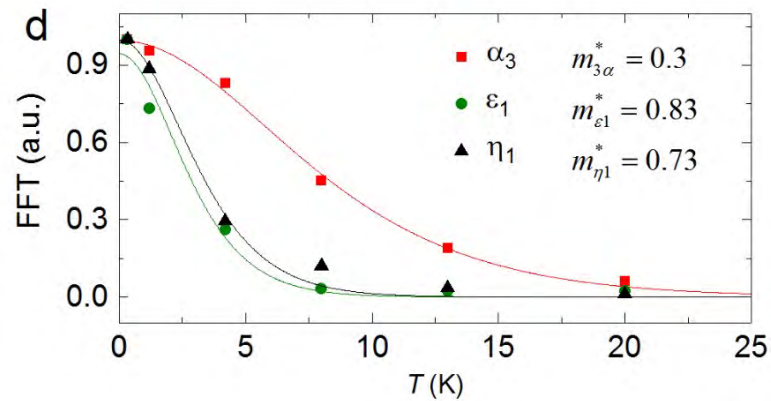
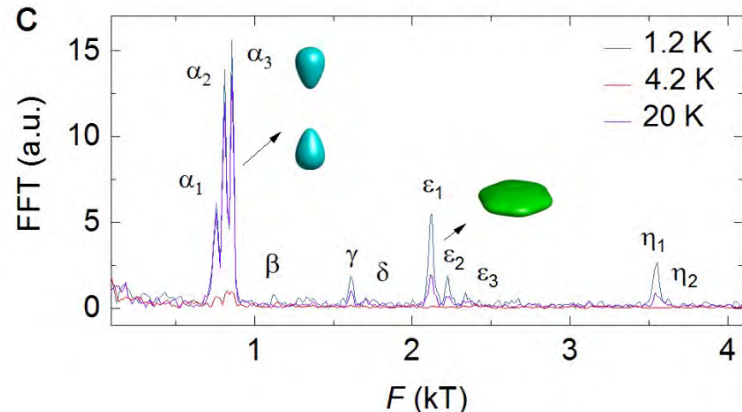
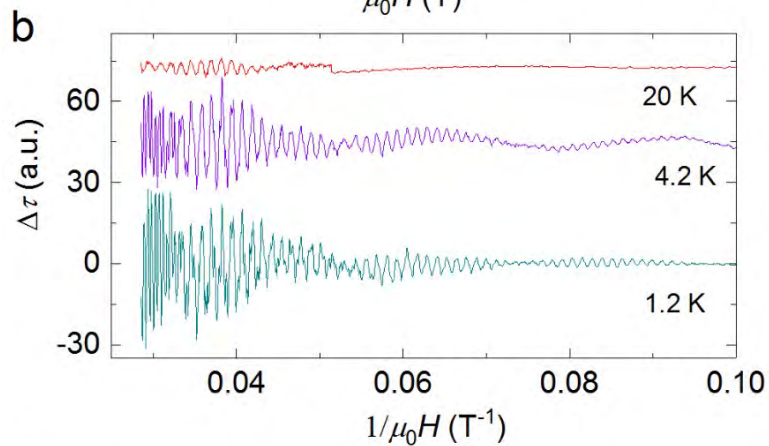
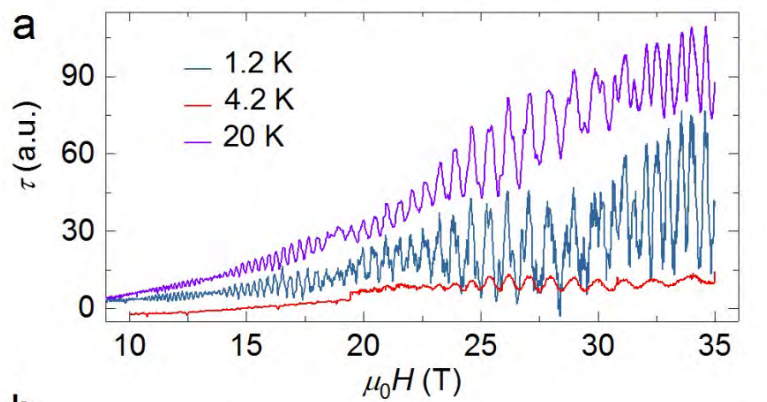
$$3.2 \times 10^{22} \text{ cm}^{-3} \text{ at 2K}$$

Experiment and calculation have the same order of magnitude

Charge carriers are mainly from the open Fermi surface

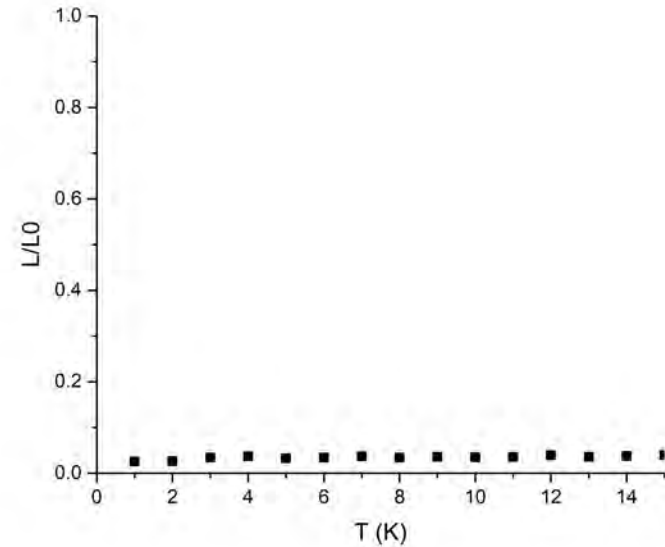
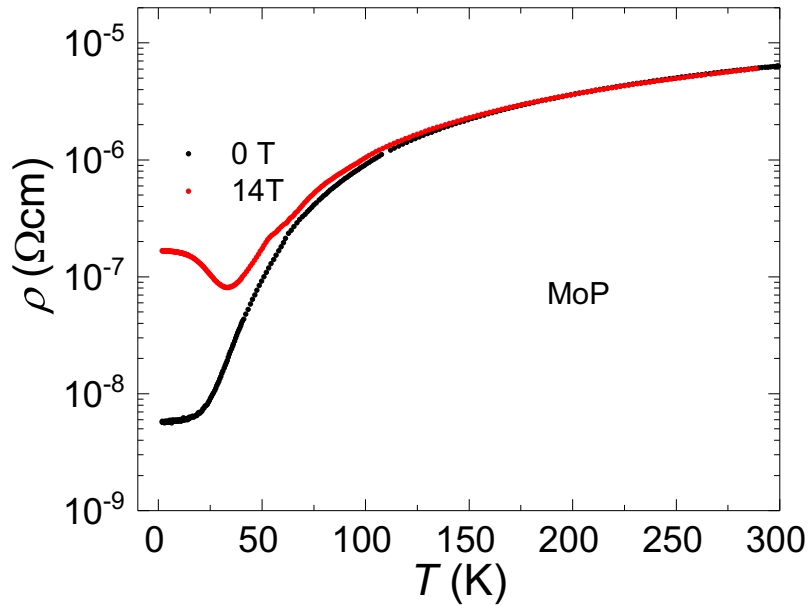


Quantum Oscillations





Hydrodynamic



- A strong violation of the Wiedemann-Franz law
- The Lorentz

$$L \equiv \frac{\kappa}{\sigma T} = \frac{\pi^2}{3} \equiv L_0$$

Compound	ρ (Ωcm)	l (μm)	μ ($\text{cm}^2\text{V}^{-1}\text{s}^{-1}$)	n (cm^{-3})
MoP	6×10^{-9}	11	2.4×10^4	2.9×10^{22}
WP ₂	3×10^{-9}	530	4×10^6	5×10^{20}
WC	0.35×10^{-6}		$\sim 1 \times 10^4$	4×10^{20}
PtCoO ₂	40×10^{-9}	5	0.7×10^4	2.2×10^{22}
PdCoO ₂	9×10^{-9}	20	2.8×10^4	2.4×10^{22}



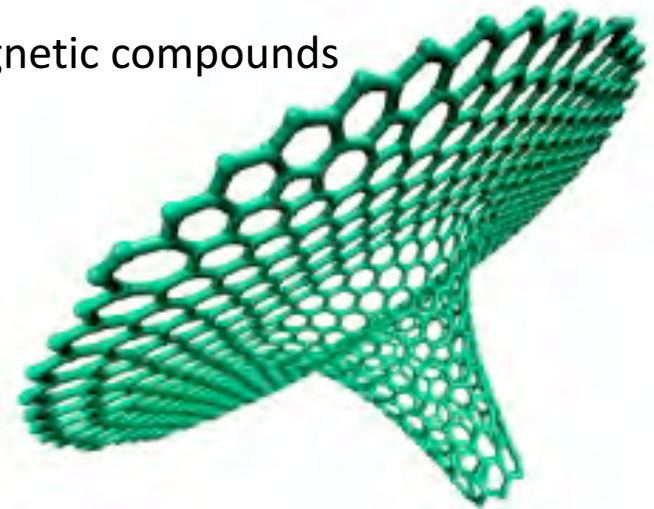
Summary

Fermi arcs and a chiral anomaly in magneto-transport are signatures of Weyl semimetals

We found new magneto thermal transport properties in Weyl semimetals and topological metals which can be explained by hydrodynamic flow of the electrons

These phenomena are also found in magnetic compounds

... much more to do!



arXiv:1511.07672v1



Single Crystals available

BaCr ₂ As ₂	AlPt	MoSe ₂ -xTex	Ag ₂ Se	YPtBi	YbMnBi ₂
BaCrFeAs ₂	GdAs	MoTe ₂ -xSex	IrO ₂	NdPtBi	Ni ₂ Mn _{1.4} In _{0.6}
	CoSi	MoTe ₂ (T'/2H)	OsO ₂	GdPtBi	YFe ₄ Ge ₂
CaPd ₃ O ₄			ReO ₂	YbPtBi	
SrPd ₃ O ₄	MoP	PtTe ₂	WP ₂	ScPdBi	Mn _{1.4} PtSn
BaBiO ₃	WP	PtSe ₂	MoP ₂	YPdBi	
		PdTe ₂		ErPdBi	CuMnSb
Bi ₂ Te ₂ Se	TaP	PdSe ₂	VAI ₃	GdAuPb	CuMnAs
Bi ₂ Te ₃	NbP	OsTe ₂	Mn ₃ Ge	TmAuPb	
Bi ₂ Se ₃	NbAs	RhTe ₂	Mn ₃ Ir	AuSmPb	Co ₂ Ti _{0.5} V _{0.5} Sn
BiSbTe ₂ S	TaAs	TaTe ₂	Mn ₃ Rh	AuPrPb	Co ₂ VAI _{0.5} Si _{0.5}
BiTel	NbP-Mo	NbTe ₂	Mn ₃ Pt	AuNdPb	Co ₂ Ti _{0.5} V _{0.5} Si
BiTeBr	NbP-Cr	WSe ₂	OsSn	Ni ₂ Sr	Mn ₂ CoGa
BiTeCl	TaP-Mo	HfTe ₅	OsSn	AuLuSn	Co ₂ MnGa
	TaAsP	MoTe ₂		AuYSn	Co ₂ Al ₉
LaBi, LaSb		TaS ₂		ErAuSn	Co ₂ MnAl
GdBi, GdSb	CrNb ₃ S ₆	PdSb ₂		EuAuBi	Co ₂ VGa _{0.5} Si _{0.5}
	V ₃ S ₄	Cu _x WTe ₂			Co ₂ TiSn
HfSiS	Cd ₃ As ₂	FexWTe ₂		CaAgAs	Co ₂ VGa
		WTe ₂			Co ₂ V _{0.8} Mn _{0.2} Ga
Bi ₄ I ₄	MnP	Co _{0.4} TaS ₂		KMgSb	CoFeMnSi
	MnAs	Fe _{0.4} TaS ₂		KMgBi	
BaSn ₂				KHgSb	
				KHgBi	
				LiZnAs	
				LiZnSb	

Thank you!

